Physics – Uspekhi **60** (5) 472 – 489 (2017)

REVIEWS OF TOPICAL PROBLEMS PACS numbers: **91.30. – f**, 91.30.Px

Scale invariance of shallow seismicity and the prognostic signatures of earthquakes

I R Stakhovsky

DOI: https://doi.org/10.3367/UFNe.2016.09.037970

Contents

Abstract. The results of seismic investigations based on methods of the theory of nonequilibrium processes and self-similarity theory have shown that a shallow earthquake can be treated as a critical transition that occurs during the evolution of a nonequilibrium seismogenic system and is preceded by phenomena such as the scale invariance of spatiotemporal seismic structures. The implication is that seismicity can be interpreted as a purely multifractal process. Modeling the focal domain as a fractal cluster of microcracks allows formulating the prognostic signatures of earthquakes actually observed in seismic data. Seismic scaling permits monitoring the state of a seismogenic system as it approaches instability.

Keywords: seismicity, multifractal measure, prognostic signatures of earthquakes, seismic kinetics, scaling, fault field, seismic field, scaling correspondence

1. Introduction

A shallow earthquake is a natural phenomenon that is extremely difficult to explore and which to date has lacked an adequate description, not only at the theoretical but also at the phenomenological level. The preparation processes of shallow earthquakes can hardly be classified as the subject of a single branch of science or even interdisciplinary branches. Both seismology and geophysics contribute to studies of shallow earthquakes [1, 2]; during a rather long period of time, earthquakes were viewed as acts of mechanical failure in rock material [3]. With the appearance of the kinetic strength concept and quantum models for the breakup of chemical bonds in crystals, the failure proper of crystal media (the rock) turned out to be in the scope of questions treated by physical chemistry and quantum chemistry [4, 5], while the phenomenon of magnetoplasticity led to interest on the part of chemical physics [6]. Nevertheless, current progress in research on processes leading to shallow earthquakes is related largely to advances in the theory of nonequilibrium processes, i.e., nonlinear dynamics and catastrophe theory [7, 8], the multifractal measure theory [9, 10], and the theory of dissipative structures and self-organization [11, 12].

In the framework of the theory of nonequilibrium processes, many specific features of seismicity in the crust find a natural explanation, and many seismic objects obtain a natural description. The development of nonlinear dynamics methods, uniform for nonequilibrium systems of various natures, allows understanding the processes of earthquake development more deeply than through the direct study of seismic objects by classical physics methods. For example, a set of new nontrivial properties of seismicity is revealed by catastrophe theory methods [13]; no less fruitful in exploring seismicity is the concept of self-organized criticality in complex systems [14]. Even though the creation of a universal, complete, and self-consistent theory of nonequilibrium processes is still ahead, the role of the already known laws of nonequilibrium system evolution in seismic processes is so obvious today and the number of experimental and modeling papers devoted to the topic is so large that the time is ripe for some (even if preliminary) generalizations.

I R Stakhovsky Schmidt Institute of Physics of the Earth, Russian Academy of Sciences,
ul. Bol'shaya Gruzinskaya 10/1, str. 1, 123242 Moscow, Russian Federation
E-mail: stakhov@ifz.ru

Received 5 July 2016, revised 8 September 2016
Uspekhi Fizicheskikh Nauk **187** (5) 505 – 524 (2017)
DOI: https://doi.org/10.3367/UFNr.2016.09.037970
Translated by S D Danilov; edited by A M Semikhatov

This review is devoted to studies of the fundamental property of crustal seismicity that follows from the essentially nonequilibrium, dissipative character of this process — the scale-invariance of spatiotemporal seismic structures. This property, empirically studied at present in hundreds of experimental and modeling papers and in studies analyzing seismic catalogues, indicates that earthquakes cannot be considered a mechanical phenomenon any longer: the solutions of partial differential equations characteristic of classical mechanics lack scale invariance (self-similarity), or the scale invariance is present in them only in trivial forms. The process of rock failure (which includes seismicity) is characterized by a huge scale range: the ratio of the length of microcracks forming in rock to the length of ruptures arising in earthquakes reaches 2^{-50}, whereas classical physics is bound to explore predominantly a single-scale level of any process. Many macrophysical properties of seismicity, by virtue of its scale invariance, stem from events at the microlevel, and ignoring this fact leads to qualitative and analytic drawbacks. Scale invariance is simultaneously a 'microscope' revealing information on microscopic processes from which earthquakes start to develop in Earth's interior and a tool to achieve statistical generalization of a seismic process as a whole.

Self-similarity occurs as a consequence of self-organization in nonequilibrium systems, which, as applied to seismicity, implies the self-organization of a seismogenic system. Historically, the theory of self-similarity (the theory of multifractal measures) was developed in close connection with studies of both mathematical objects such as strange attractors [15] and nonequilibrium physical–chemical processes such as turbulence [16], coagulation [17], or even the origin and distribution of mineral resources in Earth's crust [9]. The so-called thermodynamic analogies, well known from the theory of multifractal measures [9, 18], allow providing the mathematical equations with a physical meaning. The series of nonequilibrium natural processes presenting practical examples of scale invariance also includes seismicity as 'turbulence of solids' [19], which motivates the consideration of seismic statistics in terms of the self-similarity theory.

In what follows, the term 'seismicity' implies the seismicity in the crust, i.e., the shallow-focus seismicity in plates, whose mechanism can be related to the self-organization and brittle fracture of multicomponent rock. Such is, in particular, the seismicity in the southern California, Transbaikal, and northern Anatolia.The mechanism of deep-focus earthquakes observed in regions such as New Zealand, the Tonga Islands, or the Sea of Okhotsk can be different. Physical processes leading to deep-focus seismicity are poorly known at present: they call for further research.

2. Scale invariance in nonequilibrium multicomponent systems

2.1 Theory of dissipative structures

The theory of dissipative structures created by the Nobel Prize winner Prigogine (and the Brussels School of physical chemists led by him until 2003) laid the foundations of modern views on dissipative nonequilibrium processes and introduced the terminology used presently in many branches of science [11,12]. The theory considers the evolution of open dissipative systems that are in states far from equilibrium and are composed of metastable fluctuating subsystems. It can easily be seen that such a general definition includes a very broad class of systems, in particular, many natural systems. If more energy enters an open dissipative system than this system can accumulate, it sheds off the energy at 'sink' points or points of dissipation. The sets of dissipation points form spatiotemporal dissipative structures.

In 1945, Prigogine proved a theorem on the minimum of entropy production in open systems [20]. Following Prigogine, we let S denote the entropy of an open system, $\mathrm{d_e}S$ denote the entropy transport through the boundaries of the system, and $\mathrm{d_i}S$ denote the entropy production inside the system. For stationary states,

$$\frac{\mathrm{d}S}{\mathrm{d}t} = \frac{\mathrm{d_e}S}{\mathrm{d}t} + \frac{\mathrm{d_i}S}{\mathrm{d}t} = 0\,, \tag{1}$$

where t is the time. If the boundary conditions prevent the system from reaching thermodynamic equilibrium (zero entropy production), the system moves to the state of 'minimum dissipation':

$$\frac{\partial}{\partial \mathbf{X}}\left(\frac{\mathrm{d_i}S}{\mathrm{d}t}\right) = 0\,. \tag{2}$$

Here, $\mathbf{X}$ is a generalized force. The principle of the entropy production minimum is valid only in the vicinity of equilibrium, i.e., in weekly nonequilibrium systems. In strongly nonequilibrium states, the characteristics of the system can change radically: the system evolution is realized via a sequence of bifurcations, in the vicinity of which the amplitudes of fluctuations can exceed the mean values of system parameters. Thus, the characteristics of the system start to be determined by fluctuations. Among the consequences of strongly nonequilibrium states is the appearance of dissipative structures and self-organization. Prigogine defines self-organization as follows: "The self-organization is the choice of one of solutions appearing at the bifurcation point, defined by the probability laws. A strongly nonequilibrium self-organization leads to an increase in complexity" [12].

On the one hand, the realization of a future state of a strongly nonequilibrium dissipative system via a sequence of bifurcations makes the evolution of the system irreversible, which, in particular, rules out the description of the system in terms of deterministic mechanics allowing time reversal ($t \to -t$), for example, the description of deformations in a seismogenic medium in terms of elasticity theory. However, even though it may seem strange, thermodynamic fluctuations play a constructive role in the theory of dissipative structures: in multi-component systems they are the cause of long-range correlations and self-organization processes. A system composed of metastable subsystems in a strongly nonequilibrium state starts to evolve as a whole, i.e., in essence, it passes into a more ordered state or even a sequence of more ordered states. The classical formulation of the second law of thermodynamics for nonequilibrium but closed systems notwithstanding, in open strongly nonequilibrium dissipative systems, the entropy can decrease in the process of self-organization, which constitutes the contents of the so-called S-theorem [21]. Beyond condition (2), open systems that host irreversible fluctuating processes (i.e., essentially random processes) give rise to high levels of organization, to dissipative structures. The entropy, considered to be the measure of disorder in traditional physics, can become a source of order in strongly nonequilibrium systems.

On the other hand, the realization of a future state of a strongly nonequilibrium dissipative system via a sequence of bifurcations changes the notion of time, making it richer conceptually. Prigogine introduces the concept of 'internal' time of a nonequilibrium system, which is the measure of the change in the thermodynamic entropy. The internal time is introduced as an operator "similar to the operators that correspond to various physical quantities in quantum mechanics" [12], and the measured times of qualitative changes in the system are defined by the eigenvalues of this operator. The astronomical time "becomes the mean of the operator of new time" [12]. Put differently, the internal time coincides on average with the astronomical time, but can differ from it in intervals of instability.

Self-organization occurs only in systems with a high level of nonlinearity, in dissipative nonequilibrium systems evolving far beyond the realm where the laws of classical physics are applicable. Moreover, for the emergence of dissipative structures, it is commonly required that the system size exceed some critical value, i.e., be sufficiently large. A seismogenic system is an example. The crustal seismicity should in all probability be understood precisely as a result of self-organization in the material of Earth's crust, and this determines the tools suitable for its exploration.

2.2 Concept of self-organization of multicomponent systems in a critical state

Prigogine's paradigm of self-organization as a spontaneous transition from chaos to order and the formation of dissipative structures in open nonlinear media proved to be extremely fruitful. In 1987, a model of such a spontaneous transition was proposed in [22], which has become known as the sandpile model. If a stream of sand falls on a plane, then, when the pile reaches a critical slope with the plane, a steady state sets in: 'avalanches' are shed from the pile, new sand compensates the mass lost to the 'avalanches', and the shape of the pile stops changing. The number of avalanches N containing s sand particles then satisfies the relation

$$N(s) \propto s^{-\alpha}\,, \tag{3}$$

where α is a constant. Property (3) turned out to be universal for a wide class of nonequilibrium systems. The authors of Ref. [22] called it *self-organized criticality* (SOC). The model can be easily implemented numerically, which stimulated its study by many authors [23–25].

The concept of SOC reduces the diversity of complex processes, including those observed in Nature, to a simple model containing power-law dependence (3), with the relevant quantities re-interpreted differently in each particular case. The authors of [22] named seismicity as the first example of a natural process demonstrating self-organization in a critical state. This is because seismicity obeys the firmly established Gutenberg–Richter empirical law, which can be written in the 'energy form' as

$$E(N) \propto N^{-\beta}\,, \tag{4}$$

where N is the number of earthquakes with the energy E and β a constant (from physical considerations, the power law in (4) is written for a dimensionless quantity). Many papers followed where the seismic process was explored from the standpoint of the self-organization of complex systems in a critical state [26–28].

The concept of SOC found use in many branches of science [29]. In spite of attempts undertaken previously to shape it as a classical theory (in particular, with the help of operator formalism and group theory [29, 30]), SOC remains 'library of computer models', formally united by mathematical analogies. The explanation is that SOC is oriented to the modeling of principally nonintegrable systems. Integrable dynamic systems are isomorphic to free, noninteracting particles or can be decomposed into noninteracting subsystems. Self-organization in such systems is impossible and emerges only in those systems where the characteristics of the whole and its parts do not coincide.

Power-law distributions (3) and (4) serve as a statistical expression of scale invariance. In real systems, the scale invariance takes much more complex forms, but in virtually all cases indicates that the system reaches its critical state owing to self-organization. The power-law distributions (or, as they are sometimes called, distributions with a 'heavy tail') give a high probability of catastrophic events, substantially exceeding that for normal or exponential distributions. In this sense, scale-invariant structures are frequently related to the hazard of catastrophes in the system and can serve as an indicator of this hazard on their own.

In the seismic process, the dissipative points are the hypocenters of earthquakes. The sets of hypocenters (or epicenters if two-dimensional distributions are considered) can be regarded as dissipative structures of a seismogenic system. They emerge spontaneously as the result of self-organization in Earth's crust material, whereas their self-organization leads to their scale invariance (self-similarity). Luckily, the great majority of earthquakes are too weak to create serious damage to the productive activity of humankind. However, obeying power law (4), Earth's crust in seismically active regions turns out to be capable of inducing rare but catastrophic events. The scale invariance of seismic (i.e., dissipative) structures can therefore be a warning of an approaching danger, i.e., the transition of the crust material to the critical state.

2.3 Theory of multifractal measures

The theory of multifractal measures appeared as a mathematical tool to describe the general case of self-similarity arising in numerous mathematical problems and in natural objects that are in a critical state. The birth of fractal geometry can be dated back to 1982 when the book by Mandelbrot, *Fractal geometry of nature* [31], was published. Later on, the general theory of self-similarity (the theory of fractal measures) was elaborated in papers by Frisch and Parisi [32], Grassberger [15], Halsey [33], Mandelbrot [9], and Schertzer and Lovejoy [34, 35].

We give brief explanations of the theory together with definitions of the terms used in what follows. Let F be a bounded domain in a D-dimensional Euclidean space. We assume that a (probability) measure P is defined on F. We cover F with a grid of identical D-dimensional rectangular boxes and let p_i denote the content of measure P in the ith box. Carrying out a renormalization of the measure (scale transformation), we can vary the spatial resolution by combining several boxes of the original grid into a larger box on a new scale (for the development of general renormalization group theory, Wilson [36] was awarded the

Nobel Prize). In studies of physical systems, the measure P can, for example, characterize the probability distribution of the appearance of dissipative points as the system passes to the critical state. If the geometrical properties of a critical system are the same on all scales, the critical state is a fixed point of the scale transformation.

We introduce the partition function

$$Z_q(r) = \sum_{i=1}^{N} p_i^q(r)\,, \quad q \in \{-\infty, +\infty\}\,, \tag{5}$$

where r is the size of the scaling grid box, N is the number of boxes that are not empty, and q is the order of the measure moment. For a self-similar measure, the partition function has a power-law dependence on the scale

$$\sum_{i=1}^{N} p_i^q(r) \propto r^{-d}\,. \tag{6}$$

If relation (6) holds, the power-law exponent d is a function of q, i.e., $d = \tau(q)$, where $\tau(q)$ is called the cumulant generating function. In the limit $r \to 0$, it can be defined as

$$\tau(q) = \lim_{r\to 0} \frac{\ln\left(\sum_{i=1}^{N} p_i^q(r)\right)}{\ln(1/r)}\,. \tag{7}$$

In the scaling analysis of physical systems, the function $\tau(q)$ can be deduced directly from experimental results. For example, we assume that in exploring a stochastic process in the course of some experiment, numerical or physical, the result is obtained as some set A, whose elements can be of any physical nature. We also assume that the elements of the set belong to a finite-dimensional Euclidean space $A \subset R^D$ $(D = 1, 2, 3, \ldots)$. We define the measure P as a function of the set A such that it characterizes the probability of detecting the elements of the set in a given region of space. We use the following notation: A_i is the number of elements of the set A in the ith box of the scaling grid and N_A is the full number of set elements. The probability p_i of the elements of A to be in the ith box (or the content of the measure P in the ith box) can be approximated by the ratio $p_i = A_i/N_A$, and we hence have the equality $\sum_{i=1}^{N} p_i = 1$. By renormalization, we can consider the set A on different scale levels, which, in particular, allows formalizing the notion of 'scale level'. The value of $\tau(q)$ for a given q can be estimated as the coefficient of the linear regression $\ln\left(\sum_{i=1}^{N} p_i^q(r)\right)$ to $\ln r$.

The spectrum of generalized fractal dimensions of a self-similar measure is the function [15]

$$D_q = \frac{\tau(q)}{1-q} = \frac{1}{q-1} \lim_{r\to 0} \frac{\ln\left(\sum_{i=1}^{N} p_i^q(r)\right)}{\ln r}\,. \tag{8}$$

The generalized dimensions are characterized by monotonicity: $D_{q1} \leqslant D_{q2}$ for $q_1 \geqslant q_2$. Just like $\tau(q)$, the function D_q is defined on the infinite interval from $q = -\infty$ to $q = \infty$. As we see, fractal dimensions D_q can be fractional.

For $q = 0$, D_0 is called the monofractal dimension or simply the fractal dimension $d_{\rm f}$ of the set A (and also the measure P induced by the set A). The fractal measure has the following properties:

— if the set A is everywhere dense in R^D, then $d_{\rm f} = D$; for example, a smooth line has dimension 1 and a smooth surface has dimension 2, and so on;

— if $A_1 \subset A_2$, then $d_{\rm f}(A_2) \geqslant d_{\rm f}(A_1)$;

— if $A_1, A_2, A_3, \ldots$ is a countable number of sets N, then

$$d_{\rm f}\left(\bigcup_{i=1}^{N} A_i\right) = \sup_i \{d_{\rm f}(A_i)\}\,;$$

— if A is finite, then $d_{\rm f} = 0$.

The last property makes it impossible to rigorously apply the notion of fractal dimension to the analysis of experiments, the result of which can only be a finite set. Because direct computations with infinities are impossible, the scaling parameters computed by experimental data have the meaning of a sampling dimension determined in a finite interval of scales or with the help of finite sampling.

If the set A is characterized by a single value of the fractal dimension $d_{\rm f}$, it is called a homogeneous (ideal) fractal (monofractal). Mandelbrot defines the fractal as a set for which its fractal dimension is strictly larger than its topological dimension [31] (admitting that such a definition is possibly too stringent). Monofractals are related to the simplest nontrivial self-similar sets that preserve their form for central affine scale transformations

$$\mathbf{X}' = C\mathbf{X}\,, \tag{9}$$

where $\mathbf{X} = (x_1, \ldots, x_n)^{\rm T}$ is the column vector of the coordinates of the set elements before the transformation, $\mathbf{X}' = (x_1', \ldots, x_n')^{\rm T}$ is the column vector of the coordinates after the transformation, and C is the operator of scale change. If C is a positive real number, then relation (9) defines a group of self-similarly transformations. The operator of scale change can be given a more general interpretation [see Eqns (19)–(21)].

A monofractal is not the most realistic model of the geometry (more precisely, topology) of real objects. In general, a self-similar set is a superposition of fractal subsets characterized by their own values of fractal dimensions. For an infinite number of subsets, the structure of the set containing them is described by a D_q spectrum constructed with the help of a measure induced by the set.

An alternative way of describing the structure of a self-similar measure is the computation of the scale-invariant function $f(a)$ [33]. For self-similar measures (fields), the condition

$$p_i \propto r^{a_i} \tag{10}$$

holds, where the singularity index a_i depends on the position of the ith box. The singularity index a_i characterizes the local self-similarity of the field studied. In [33], a measure P is called multifractal if it also satisfies the global self-similarity condition

$$\sum N_a(r) \propto \rho(a, r)\, r^{-f(a)}\,, \tag{11}$$

where $\sum N_a(r)$ is the number of boxes with the common value of a and $\rho(a, r)$ is a function slowly varying in a and r such that

$$\frac{\ln \rho(a, r)}{\ln(1/r)} \underset{r\to 0}{\longrightarrow} 0\,. \tag{12}$$

The prefactor $\rho(a, r)$ serves to correct relation (11) for r far from zero and can be used to estimate the degree of lacunarity of the object. The function $f(a)$ is known as the singularity spectrum of a multifractal measure.

From Eqn (10), we find (if the limit exists)

$$a_i = \lim_{r \to 0} \frac{\ln p_i}{\ln r} \,. \tag{13}$$

It follows from Eqn (11) that

$$f(a) = -\lim_{r \to 0} \frac{\ln \sum N_a}{\ln r} \,. \tag{14}$$

It can be shown that the spectrum of generalized fractal dimension D_q is related to the singularity spectrum $f(a)$ by the Legendre transform [9]

$$a = \frac{\mathrm{d}\big[(q-1)D_q\big]}{\mathrm{d}q} \,, \tag{15}$$

$$f(a) = aq + (1-q)D_q \,. \tag{16}$$

The Legendre transform allows one to practically compute the singularity spectrum by the scaling analysis of physical objects. We note, however, that the Legendre transform, which includes a set of smoothing operations, is sensitive to the finite grid resolution and inadequate sampling of the data. As a result, the sought weak perturbations of $\tau(q)$ can be lost in the process of numerical computations. Distortions or linearization of $\tau(q)$ can also be caused by the poor original data. For small values of $|q|$, low-amplitude oscillations of the cumulant generating function can be related to the presence of noise in the object being explored and noise in the measuring system, where its appearance is often unavoidable. To compute $f(a)$ without resorting to the Legendre transform, an algorithm of direct computation of the singularity spectrum was proposed [37]. Other algorithms for finding the scale-invariant function $f(a)$ were proposed, for example, with the help of constructing a histogram of the distribution of the ratio $\ln\left(\sum_a N_a\right)/\ln(1/r)$ and subsequent parabolic interpolation of the histogram [38]. Each algorithm has its applicability domain, which requires care in using them because the limits in Eqns (8), (13), and (14) can be obtained in experimental data processing only approximately.

The cumulant generating function has no extrema. An extremum of $f(a)$ equals the monofractal dimension of the measure $f_{\max}(a) = D_0$. The dimensions D_1 and D_2 are commonly called the respective entropy and correlation dimensions of the measure being explored and the supporting set. When the set being explored is monofractal, the entropy and correlation dimensions of the measure induced by the set, as well as other dimensions, coincide with the monofractal dimension of the supporting set. Multifractal measures are not differentiable; accordingly, the probability given by the content of the measure cannot be related to a probability density.

Hence, if a multifractal measure P is supported by a set A that can be represented as a union of fractal subsets A_a with fractal dimensions a,

$$A = \bigcup_a A_a \,, \tag{17}$$

then the topological properties of the measure can be described with the help of scale-invariant functions such as the spectrum of generalized fractal dimensions D_q or the singularity spectrum $f(a)$.

The theory by Schertzer and Lovejoy [34, 35] is based on the notion of codimension, i.e., the number completing the fractal dimension to the dimension of the embedding space. A $(\gamma, c(\gamma))$ notation is used in [34, 35] which the authors call 'turbulent', in contrast to the notation $(a, f(a))$ used above, which they call the 'attractor' notation. From the standpoint of exploring objects in physical space (i.e., objects existing in a single realization), these notations are equivalent. The above authors introduced the notion of 'generalized scale invariance' [35]. As the scale transformation operation, they use the map

$$B' = T_\lambda B \,, \tag{18}$$

where B and B' are the coordinates of the elements of the set before and after the transformation, and T_λ is the operator of scale change, which is written as

$$T_\lambda = \lambda^{-G} \,, \tag{19}$$

where λ is a dimensionless scale factor. In the case of a linear scale transformation, the power-law exponent G in Eqn (19) is expressed in terms of the sums of matrices known from the algebra of quaternions (we limit ourselves to considering a two-dimensional (2D) space),

$$G = a\hat{1} + b\hat{I} + c\hat{J} + d\hat{K} \,, \tag{20}$$

where $\hat{1}$, $\hat{I}$, $\hat{J}$, $\hat{K}$ are analogs of the Pauli matrices,

$$\begin{aligned} \hat{1} &= \begin{pmatrix} 1 & 0 \\ 0 & 1 \end{pmatrix}, \quad \hat{I} = \begin{pmatrix} 0 & -1 \\ 1 & 0 \end{pmatrix}, \\ \hat{J} &= \begin{pmatrix} 0 & 1 \\ 1 & 0 \end{pmatrix}, \quad \hat{K} = \begin{pmatrix} -1 & 0 \\ 0 & 1 \end{pmatrix}, \end{aligned} \tag{21}$$

and a, b, c, and d are scale factors. In particular, in the case of a linear anisotropic scale transformation, the shape of the box becomes a function of the scale. We note that the scale transform can be nonlinear in general.

The fractal description of physical systems is in essence a statistical description, which can be compared to the thermodynamic description in terms of ensembles. The function $f(a)$ in the theory of multifractal measures plays a role that is analogous to that of entropy in thermodynamics [18]. Such a comparison is in no way formal because by its physical sense it reflects the aim of both thermodynamics and the theory of fractals to describe multicomponent systems. It should be kept in mind that the possibility of a geometrical formulation of thermodynamics was already demonstrated in studies by Gibbs in the early 20th century [39]. Whereas classical physics was always understood as the science of energy transformations, nonequilibrium physics is rather the science of transformations of structures.

The thermodynamic analogies in the theory of multifractal measures ($f(a) \sim -S$, $q \sim T^{-1}$, and $a \sim -E$, where S is the entropy, T is the absolute temperature, and E is the Gibbs free energy) were of course noticed immediately by the author of the theory of dissipative structures. In book [11], Prigogine notes that the research on nonequilibrium structures required an extended functional space from the very beginning, and the lack of suitable mathematical tools created 'technical' difficulties. The strong instability of nonequilibrium processes destroys the trajectories of the system in phase space (even for an arbitrarily accurate specification of the initial conditions), and a statistical description emerges as the only possible one. Fractal geometry provided the theory of dissipative structures with the sought functional tools. In the terminology proposed by Mandelbrot, dissipative structures can be called structures possessing fractal organization, which led Prigogine to the conclusion that ``Fractals play a decisive role in understanding the laws of nature'' [11].

3. Scale invariance of disjoint structures in Earth's crust and seismicity

3.1 Real structures

The appearance of fractal geometry and the development of computer algorithms for experimental data processing led to a rapid increase in the number of works exploring self-similarity in natural objects. It turned out that many natural processes and geometric forms taken by natural systems are self-similar, which literally confirmed the main position of the dissipative system theory: Nature is created via non-equilibrium processes and is being recreated by them presently. Since the mid-1980s, research has been carried out on spatiotemporal self-similar structures occurring through the fracture of polycrystalline rock and seismicity. Presently, it can be stated that experimenters succeeded in studying the geometry of rock failure in virtually the entire range where it takes place. The experimental results, given their large number and good reproducibility, leave no doubts that scale symmetry is a fundamental attribute of rock failure.

The lowest-scale level of crack formation is determined by the possibility of distinguishing between microcracks and point defects in crystals, which corresponds to crack lengths of $10^{-9}-10^{-7}$ m. With the help of direct X-ray and electron scanning microscopy measurements and small-angle neutron scattering, it was repeatedly shown that microcracks already form sets of scale-invariant, fractal structures at the level of the crystal lattice [40–44]. In all probability, this implies that spatial distributions of point defects in crystals also obey multifractal statistics; however, it is still difficult to answer this question definitively because of the difficulty in carrying out direct observations.

The next scale level in studies of failure is the one set by the possibilities of optical microscopy and the method of acoustical emission (the length of cracks is $10^{-6}-10^{-3}$ m). The failure is typically realized as a result of loading the samples of rock in laboratory presses. Macrocharacteristics of fractures in such experiments can depend on the type of rock, its water content, the stiffness of the loading machine, the magnitude of hydrostatic pressure, or the speed of loading, but the spatial distribution of cracks in the sample practically always stays fractal and scale-invariant. The number of papers in this domain is also rather large, and we mention only some of them [45–49].

A higher scale level of failure is the geophysical one, in which the spatial distribution of cracks is explored on objects such as rock damaged between the sides of seismically active faults (fault gouges), slip mirrors in rock outcrops, and other natural objects (the length of cracks is $10^{-2}-10^{2}$ m). The methods of research are luminescent or capillary defectoscopy, on-site mapping, computer analysis of photographs, and so on. The fractal character of crack distribution is also found here [50–53].

Finally, the coarsest scale level of the failure of Earth's crustal material available for studies is the level of seismically active faults explored by geographical or geological methods or with the help of aerial or satellite photography (the fault length is $10^{3}-10^{5}$ m). The fractal analysis of these objects was already carried out in the early 1990s, and some time after that it was proved that spatial distributions in Earth's crust faults demonstrate the general case of self-similarity, i.e., they show a multifractal structure organization [54–58]. We note that all cases of rock failure, just the fault structures in Earth's crust, because of their large size, can be studied in the widest scale range. Thus, in Refs [56, 57], the resolution of scale grid was $2^9 \times 2^9$. Such a scale resolution may not always be achieved, even in studies of meteorological or hydrological objects [58–60].

The presence of scaling in spatial distributions of earthquake epicenters was discovered even before the appearance of fractal geometry with the help of a method based on the correlation integral computation [61], while studies of seismicity using multifractal theory methods were begun in the 1990s [62–64]. In the mid-1990s, the multifractal character of seismic process was still under scrutiny [65], but in the time that followed a clear concept emerged that seismicity and fault formation share a common multifractal nature [66, 67]. In contemporary work, the multifractality is already understood as a fundamental property of seismicity [68–72].

Research into the self-similarity of the temporal course of seismicity — studies of temporal dissipative structures of seismic process — began in the mid-1990s [73–75]. A remark is due here. There is a certain difference between the multifractality of spatial distributions of earthquake epicenters and that of the temporal course of seismicity. Spatial seismic fields are multifractals with localized singularities. Spatial seismic fields (i.e., multifractal measures modeling the spatial distribution of earthquake epicenters) are characterized by the existence of limit (13) and repeated generation of micro-earthquakes at the same field points. In particular, this leads to the fact that spatial distributions of epicenters of paleoseismicity practically coincide with the distribution of current seismicity in regions where representative historical catalogs are available (Italy, Greece, the Caucasus, Scandinavia). In other words, spatial distributions of seismicity are described by 'geometrical' multifractals.

The temporal course of seismicity, however, does not have this property: it is characterized by another kind of multifractality. It is described by 'stochastic' multifractals for which limit (13) is absent, i.e., the temporal course of seismicity shows statistical self-similarity. The difference between geometrical and stochastic multifractals can be most conveniently explained with the help of a mathematical procedure called the multiplicative cascade (see below).

Research on self-similarity in the time evolution of seismicity actively continues today [76, 77]. There are no doubts that scale invariance is present in the temporal course of seismicity, but this leads to a natural question: are the seismic time series self-similar always or only in certain phases of seismic process? Indeed, the seismic process can be considered to be practically infinite, even though today we can explore samples of a maximum duration of 20–30 years. We try to find an answer to this question in what follows, and now summarize the results of experimental work.

The fractal organization of sets of cracks is observed for all mesoscales of failure from the micro- to the macrolevel, i.e., from the scale level of a crystal lattice to the scale of earthquakes and seismically active faults. Because of this fundamental self-similarity, the seismicity and formation of micro-cracks should be related to the same universality class [78], but the real relation between them is even deeper. The independence of the structure of failure from the scale allows us (as a substantiated assumption) to consider the formation of micro-cracks and seismicity as opposite boundaries of the scale spectrum of a unique scale-invariant process controlled by unique order parameters. We do not have any grounds to distinguish the formation of micro-cracks and seismicity on the level of complexity, the number of controlling parameters, or the geometry of the fracture, because we cannot propose any scale boundaries in the entire range between the formation of micro-cracks and seismicity. According to the data in Ref. [50], even monofractal dimensions of crack structures in the wide scale range of rock failure fit a relatively narrow range $d_{\mathrm{f}} \approx 2.6 \pm 0.11$ (for three-dimensional distributions). Rock failure preserves scale symmetry in such a wide range of scales that it is difficult to find any comparable physical process on Earth!

3.2 Some model results

The appearance of fast and powerful modern computers has allowed writing code of numerical multi-step algorithms in various models of kinetic growth, in particular, in lattice models of quasistatic fracture of structured solid bodies. In models of this kind, it is assumed that the deformation properties of the grid are described by equations of the continuum medium mechanics, and the crack growth is modeled by breaking up the grid connections. It should be remembered that the nonequilibrium state of material at the crack tip, according to the theory of dissipative structures, implies that the decisive role in fracture development is played by thermodynamic fluctuations. The fluctuating character of crack growth is reproduced by including a random number generator into the code for the selection of the crack propagation directions. The priority in this domain belongs to Refs [79, 80], which simulated fractal clusters with the shape of cavities in a grid made of triangular boxes. In [81, 82], both triangular and quadrilateral grids were used. The algorithms included a random number generator as well as fixed rules for the breakup of connections [83]. Grid models of fracture consistently simulate the generation of monofractal crack structures with the fractal dimension weakly dependent on the precise shape of the stress field. However, the respective studies dealt only with elastic material rheology. Combining the fluctuation character of fractures with a nonequilibrium state of the entire grid was achieved in Ref. [84] on a rectangular viscous–elastic grid. We turn to this model and the results obtained with its use.

The fracture (the growth in the crack cluster) in the model was realized through a stepwise algorithm of grid connection breakup as follows. We create an initial defect (one or more) in the grid by removing one (or more) connections. We introduce an orthogonal reference frame x_1, x_2, x_3 with the axes x_1 and x_2 located in the grid plane. We begin to construct the model from the equations of stress equilibrium in a deformed body: $\sigma_{ij,j} = 0$, where σ_{ij} is the stress tensor. Taking into account that the key role in the process of tectonic fracture in Earth's crust belongs to shear stresses, we relate the crack growth to the behavior of a stress deviator. Staying in the framework of a plane problem, we assume that $\sigma_{13} \neq 0$ and $\sigma_{23} \neq 0$ ($\sigma_{11} = \sigma_{22} = \sigma_{33} = \sigma_{12} = 0$). We let $\mathbf{U}$ denote the displacement vector with the components U_1, U_2, U_3, and γ_{ij} denote the strain tensor; shear deformations are then expressed as $\gamma_{13} = U_{3,1}$, $\gamma_{23} = U_{3,2}$. We consider a fracture in a nonequilibrium (viscous–elastic) grid, i.e., assume that the connections in the grid are deformed according to the rheologic equation of a Kelvin body proposed in Ref. [85] to describe tectonic deformations in Earth's crust. Then the relation between the stresses and deformations takes the form

$$\sigma_{ij} = L(2\gamma_{ij}) , \tag{22}$$

where $L = \mu + \eta\, \partial/\partial t$ is the linear viscous–elastic operator, μ is the shear modulus, η is the viscosity coefficient, and t is time.

Thus, the resolvent equation of the model takes the form

$$L(\Delta U_3) = 0 , \tag{23}$$

where Δ is the two-dimensional Laplace operator and U_3 is the displacement normal to the grid plane. For $\sigma_{ij,t} = 0$, the solution of Eqn (23) can be written as

$$U_3 = U_3^{\infty} + (U_3^0 - U_3^{\infty}) \exp\left(-t\,\frac{\mu}{\eta}\right) . \tag{24}$$

The growth of cracks in grid models is discrete and is split into 'steps', which are understood as transitions from the grid with $\mathfrak{R}$ broken connections to the state with $\mathfrak{R}+1$ broken connections, $\mathfrak{R} = 1, 2, 3, \ldots$. Let t^0 be the instant of time that correspond to the beginning of the subsequent 'step' ($t^0 = 0$), and t^{∞} be the time over which the grid passes to a state close to equilibrium. In expression (24), U_3^0 is the displacement field at the instant t^0, and U_3^{∞} is the displacement field at the instant t^{∞}. It can be shown that expression (24) is a solution of Eqn (23) if U_3^{∞} is a harmonic function, $\Delta U_3^{\infty} = 0$, satisfying boundary conditions. For numerical integration, Eqn (23) was replaced by a system of finite-difference equations based on centered second-order approximations, which was solved iteratively. The boundary conditions on the outer boundary G were given in terms of displacements, $U_3(G) = f(G)$. On the inner grid contour, the boundary conditions were set as $\sigma_{ij} n_j = 0$, where $\mathbf{n}$ is the unit vector of the outer normal to the surface.

The fluctuation character of fracture in natural conditions implies that the time and direction of fracture are determined by thermodynamic fluctuations. In the model, the fluctuations were simulated by a random number generator. It was used to select the fracture time t^{f} ($t^{\mathrm{f}} < t^{\infty}$) and the next connection to be broken from 5–10% of the most stressed connections at the instant of fracture. The process of crack cluster growth was modeled via multiple (up to 10^3 times) iterations of the procedure of grid connection breakup. The displacement field at the instant a grid connection is broken was used as the initial conditions for the next 'step' of cluster generation. The grid in this situation is *never* in the state of equilibrium: it stays permanently under the viscous deformation condition, and breaks in the next connections change the parameters of deformation.

Figure 1a shows one of the realizations of a crack cluster obtained in this computer model. The crack cluster was generated on a grid with a resolution of 100×100 from two initial defects placed at the grid center. The set of broken connections was explored by multifractal analysis methods; the spectrum of the measure $f(a)$ induced by the set of broken connections is shown in Fig. 1b.

If elastic grids give predominantly monofractal clusters (or weakly multifractal ones), the singularity spectrum $f(a)$ does not degenerate into a point in the range of scales that could be explored, i.e., the set of broken grid connections is

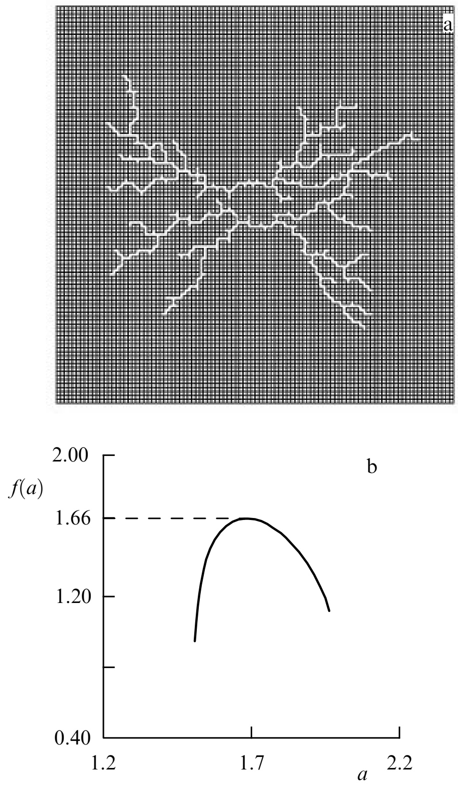

Figure 1. (a) Crack cluster generated on a 100×100 grid from two initial defects at the grid center. (b) The singularity spectrum of the multifractal measure induced by a set of broken grid connections.

not monofractal. The crack cluster demonstrates a developed multifractal scaling. The nonequilibrium grid state and the 'fluctuating' selection of the direction of crack growth (even for fixed parameters of a 'medium macrostate' $U_{3,t}(G) = 0$) are fully sufficient to obtain the structure organization of disjoint breaks in continuity observed in Earth' crust on different scales. The model describes all the diversity of elements encountered in natural systems: the convoluted character of trajectories, the branching that repeats itself infinitely, and the coalescence of cracks up to the formation of closed loops. Even though the modeled process cannot be reduced to an analytically integrable system of differential equations (the random-number generator continuously destroys the analyticity of the solution), computer simulations do capture the physical essence of the modeled object (nondynamical growth of cracks or faults in Earth's crust). Multifractal approximations of spatial crack distributions can be regarded as realistic and possibly adequate models of natural phenomena.

Processes in Nature, however, depend on many factors and involve numerous interacting fields. Fault formation and seismicity can occur simultaneously in the same natural system (accompanied by phenomena such as vertical slips of the day surface, changes in water permeability, and so on, characterized by their own scale invariance [60, 86, 87]). Are the scalings of these processes independent? This question prompts one to look for fundamentally new statistical models that would help to unravel the interaction of natural processes on a qualitatively new level.

The basis of such modeling is laid by a multiplicative cascade procedure proposed originally in Refs [88, 89] for the description of turbulence. In general, this procedure can be defined as follows. A unit D-dimensional interval undergoes a λ^D-fold subdivision, where λ is a natural number, $\lambda \geqslant 2$. At the first iteration, a positive multiplier m_j is associated with each ith element of the subdivision, and all the m_j form a finite set of numbers (initial multipliers) satisfying the conditions

$$0 \leqslant m_1 \leqslant m_2 \leqslant \ldots \leqslant m_{\lambda^D} < 1 \,, \tag{25}$$

$$\sum_{j=1}^{\lambda^D} m_j = 1 \,. \tag{26}$$

At the second iteration, each element of the subdivision once again undergoes a λ^D-fold subdivision and each newly formed element is associated with one of the initial multipliers. The result of the multiplicative procedure at the second iteration is the product of multipliers of 'parent' and 'child' elements of the subdivision. On subsequent iterations, the procedure is repeated. Let k denote the number of iterations. At the kth iteration, the ith element is associated with the product $\prod m_j^{k\varphi_j}$, where φ_j are the relative frequencies with which the multipliers m_j enter these products. Because

$$\sum_{i=1}^{\lambda^{kD}} \prod m_j^{k\varphi_j} = 1 \,, \quad k \to \infty \,, \tag{27}$$

the quantities $p_i = \prod_j m_j^{k\varphi_j}$ can be considered fractions of some multinomial measure P restricted to the ith element of the subdivision (in the ith box of the scaling grid). Each subsequent iteration modulates the measure distribution inherited from the preceding iteration, increasing the intermittency of the distribution. In the limit $k \to \infty$, the singular nowhere differentiable measure P is a multifractal also for arbitrary shuffles of 'child' boxes within the 'parent' box. Multiplicative generators give rise to an infinite diversity of self-similar distributions.

If the multipliers m_j in the cascade procedure preserve their constant values, the result is a self-similar, strictly renormalizable measure, or the so-called geometric multifractal. However, the measure P also preserves statistical self-similarity when the m_j are random numbers such that the condition

$$\sum_{j=1}^{\lambda^D} m_j = 1$$

is satisfied only as a mean over the field. In this case, the singularities of a multifractal field are no longer localized and perform a random walk over the field upon a change in scale levels. Such stochastic multifractals are called 'universal' in Refs [34, 35, 65].

The term 'universal multifractals' (not very apt, even in the opinion of the authors) should not lead to misunderstanding: the increase in the role of randomness in the measure formation leads not to generalization but to a change in the properties of the multifractal. Geometric and stochastic multifractals are related to models of physical processes with differing properties. For processes occurring in solid bodies, random walks of singularities over spatial fields and distributions are clearly not typical. Accordingly, an appropriate model for spatial distributions of fault formation and seismicity is naturally provided by geometric multifractals. Stochastic multifractals are used for mathematical modeling in meteorology and hydrology [34, 35, 60] and can be used to model the time evolution of seismicity.

We consider the structure of a two-dimensional multifractal field in more detail in the case where it can be generated by a geometric multiplicative cascade (in what follows, we use such fields to model spatial distributions of seismicity). Let a 2D (geometric) cascade contains n unique multipliers that are not connected by any relations except the conditions of measure generation (25) and (26). Each iteration creates λ^{2k} boxes of the scaling grid, representing $\Lambda(n,k)$ subsets of boxes characterized by a common value of the fractions of the measure p_i supported by them. These subsets are fractal, or more precisely, become such as $k \to \infty$. Obviously, on the first iteration, $\Lambda(n,1) = n$. For $n = 2$, as is known from the binomial measure theory, $\Lambda(2,k) = k+1$. The values of $\Lambda(n,k)$ for arbitrary n and k can be obtained with the help of the recurrence formula [90]

$$\Lambda(n,k) = \Lambda(n,k-1) + \Lambda(n-1,k)\,, \quad n > 2, \quad k > 1\,. \tag{28}$$

To describe the structure of the measure, we use the polynomial theorem known in combinatorics [91]. The fraction of the measure in grid boxes has the form

$$p_i = m_1^{\zeta_1} m_2^{\zeta_2} \ldots m_{\lambda^2}^{\zeta_{\lambda^2}}\,, \tag{29}$$

where $\zeta_1, \ldots, \zeta_{\lambda^2}$ are the numbers of occurrences of the multipliers $m_1, \ldots, m_{\lambda^2}$ in products (29). The number of boxes in each of the $\Lambda(n,k)$ subsets at the kth iteration are expressed as

$$\sum N_a = \frac{k!}{\zeta_1!\zeta_2!\ldots\zeta_{\lambda^2}!}\,, \tag{30}$$

where the exponents in Eqn (29) satisfy the condition

$$\zeta_1 + \ldots \zeta_{\lambda^2} = k\,. \tag{31}$$

The cumulant generating function is expressed in terms of the values of multipliers as

$$\tau(q) = \frac{\ln\left(\sum_{j=1}^{\lambda^2} m_j^q\right)}{\ln\lambda}\,. \tag{32}$$

Performing the Legendre transform, we obtain expressions for the spectrum of multifractal field singularities:

$$a(q) = \frac{\sum_{j=1}^{\lambda^2} m_j^q \ln m_j}{\ln\lambda \sum_{j=1}^{\lambda^2} m_j^q}\,, \tag{33}$$

$$f\big(a(q)\big) = \tau(q) + aq\,. \tag{34}$$

We continue with the model analysis and construct a model of two structurally connected multifractal processes. Let two two-dimensional multiplicative cascades Γ' and Γ'' model two multifractal fields. We assume that

(1) the cascades have the same structure, i.e., $\lambda' = \lambda''$;

(2) a one-to-one correspondence is established between the cascade multipliers, $m_j' \leftrightarrow m_j''$, i.e., only mutually related permutations of multipliers can be used to construct model fields, such that in boxes with the same number i of both scaling grids, the next multipliers of the kth iteration are in one-to-one correspondence (Fig. 2).

For all arbitrary permutations of multipliers of 'child' boxes within the 'parent' box, the multipliers of different cascades that have the same index are permuted in the process of measure generation in the same way. Let the numerical values of multipliers of these cascades m_j' and m_j'' be connected by the power-law dependence

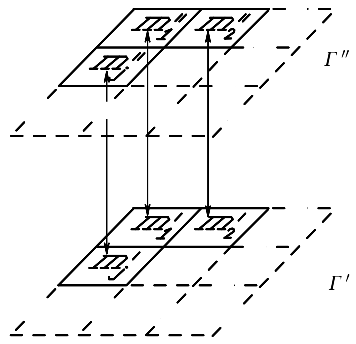

Figure 2. Distribution of model measures at the second iteration of the multiplicative process in the model of scalings correspondence using two-dimensional multiplicative cascades. The arrows point to the multipliers that are in one-to-one correspondence for any admissible permutation in the course of the subsequent iteration.

$$m_j'' = c(m_j')^\omega\,, \tag{35}$$

where c is a proportionality coefficient. In Ref. [92], it is shown that expressing the parameters of one field in terms of the parameters of the other gives the following relations for the characteristics of the fields generated by cascades:

$$a'' = \omega a' + \frac{\omega\ln\left(\sum_{j=1}^{\lambda^2} m_j'\right) - \ln\left(\sum_{j=1}^{\lambda^2}(m_j')^\omega\right)}{\ln(1/\lambda)}\,, \tag{36}$$

$$f''(a'') = f'(a')\,, \tag{37}$$

where a' and a'' are the singularity indices of the two fields at points with the same coordinates, and $f'(a')$ and $f''(a'')$ are the singularity spectra of these fields. Additionally, we obtain one more important relation:

$$\omega = \frac{a''_{\max} - a''_{\min}}{a'_{\max} - a'_{\min}}\,, \tag{38}$$

where $a'_{\max}$ and $a'_{\min}$ are the maximum and minimum values of the singularity indices for the fields generated by the cascade Γ', and $a''_{\max}$ and $a''_{\min}$ are the respective values for the singularity indices for the field generated by the cascade Γ''. We see that the scalings of the generated fields are not identical but correspond to each other, which is why this model is termed the model of correspondence in Refs [92, 93].

Seismicity gives us an example of two multifractal fields with corresponding scalings: spatial distributions of earthquake epicenters (seismic fields) and spatial distributions of seismic energy (seismoenergetic fields). We assume that the cascade Γ' generates a model of a seismic field, whereas the cascade Γ'' generates a model of a seismoenergetic field. We recall that the Gutenberg–Richter law can also be represented in the form [92]

$$E_{\text{sum}} \propto N_{\text{sum}}^{\beta}\,, \tag{39}$$

where E_{sum} is the net energy of a representative number of earthquakes, N_{sum} is their net number, and β is the exponent (its absolute value) from formula (4). The relation between the multipliers of multiplicative cascades reflecting this fact takes the form $m_j'' = c(m_j')^\beta$ [90], and expressions (36) and (38) can be written in a form that allows a direct verification

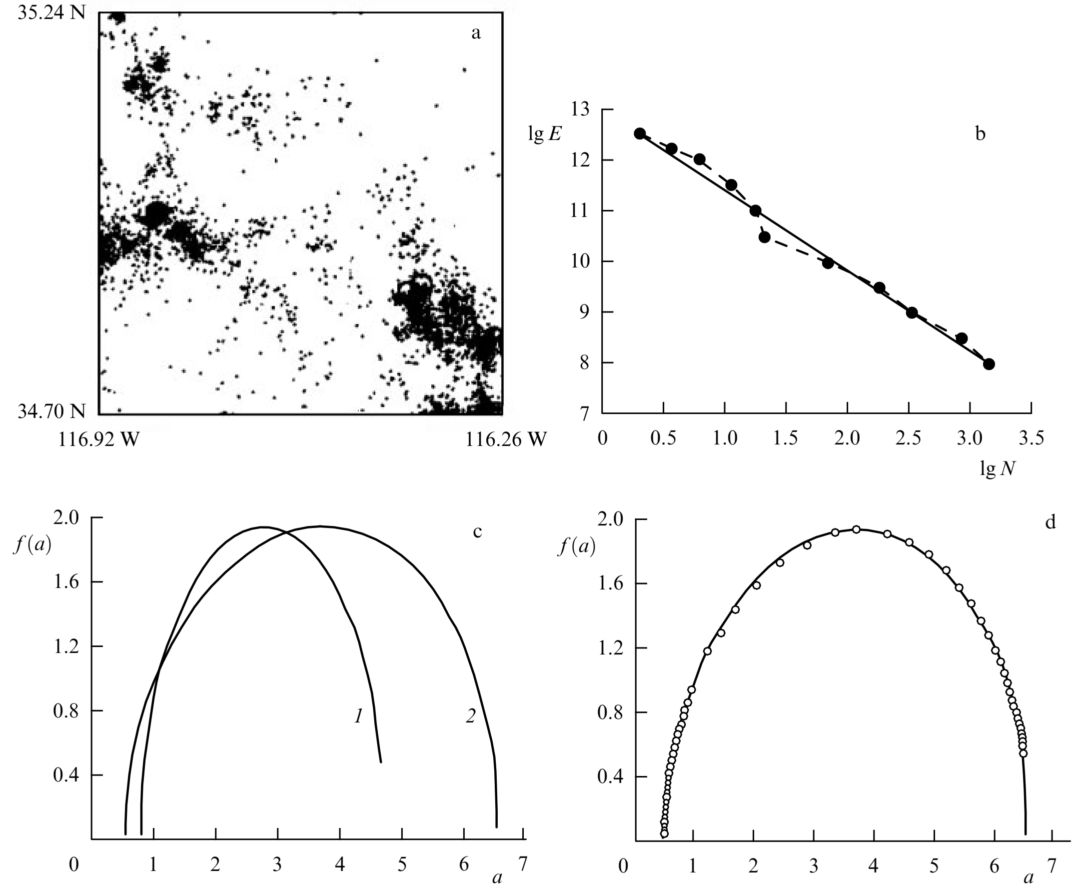

Figure 3. (a) Spatial distribution of earthquake epicenters in an area of 60×60 km^2 in the vicinity of Barstow for the period 01.01.1992–31.12.2000 in the range of magnitudes $M \geqslant 1.9$ (2946 events). Large dots mark epicenters of events with $4.5 \leqslant M \leqslant 5.2$. (b) Recurrence plot in energy form for the data sample explored here. The dots are the catalog data, the solid line is a linear regression constructed based on this data. (c) Singularity spectra of seismic (*1*) and seismoenergetic (*2*) fields. (d) The result of juxtaposing singularity spectra of the seismic field (circles) after stretching and translation transformations on the singularity spectrum of the seismoenergetic field (solid curve).

against the seismic data:

$$a'' = \beta a' + \text{const}\,, \tag{40}$$

$$\beta = \frac{a''_{\max} - a''_{\min}}{a'_{\max} - a'_{\min}}\,. \tag{41}$$

Here, a' are the singularity indices of the seismic field and a'' are the singularity indices of the seismoenergetic field. Expressions (37) and (40) show that under the scaling correspondence conditions 1 and 2 formulated above, the singularity spectrum of one field should transform into the singularity spectrum of the other one with the help of affine transformations (stretching and translations). The $f(a)$ spectra are strongly nonlinear functions and, being constructed from truly different data, they can coincide after linear transformations only when they indeed satisfy relations (37) and (40).

To test the model result, we take a set of earthquakes that occurred in a 60×60 km^2 area of Earth's crust in the vicinity of Barstow to the northwest of Los Angeles (data from the South California catalog). During the period 01.01.1992–31.12.2000 in the range of magnitudes $M \geqslant 1.9$, the catalog documents 2946 events for this region, which comprise the sampling to be explored. The spatial distribution of their epicenters is given in Fig. 3a.

Figure 3b presents the dependence of lg E on lg N based on the sampling data. The circles connected by the dashed line correspond to the catalog data and the straight line represents the linear regression computed by the least-square fit of experimental points. The regression coefficient is $\beta = -1.570\ldots$.

Figure 3c presents the $f(a)$ spectra of seismic (*1*) and seismoenergetic (*2*) fields constructed from the sampling data. Maximum and minimum values of singularity indices for the fields under study were $a'_{\min} \approx 0.770$, $a'_{\max} \approx 4.592$, $a''_{\min} \approx 0.502$, and $a''_{\max} \approx 6.495$. Using Eqn (41), we obtain the second estimate of the 'slope of the recurrence graph': $\beta \approx 1.568$.

We write dependence (40) as $a'' = \beta a' + \phi$. The coefficients β and ϕ can be estimated in different ways depending on the selected criterion of spectrum divergence. In our case, the coefficients were selected based on the construction of an auxiliary function $\hat{\tau}(q) = \beta\tau'(q) + \phi q$ and using the Kolmogorov criterion $I = \sup_{-30 \leqslant q \leqslant 30} |\tau''(q) - \hat{\tau}(q)|$ for the minimization of the maximum residual modulus between $\tau''(q)$ and $\hat{\tau}(q)$. Here, $\tau'(q)$ and $\tau''(q)$ are the cumulant generating functions for seismic and seismoenergetic fields. The estimates $\beta \approx 1.545$ and $\phi \approx -0.643$ are the result. Figure 3d shows the $f(a)$ spectrum of the seismoenergetic field and the $f(a)$ spectrum of the seismic field redrawn in agreement with expressions (37) and (40) with the above values of coefficients. After stretching and translation transformations, the $f(a)$ spectrum of the seismic field practically coincides with the $f(a)$ spectrum of the seismoenergetic field. Some insignificant discrepancies are explained by inaccuracies in constructing the $f(a)$ spectra (first of all, their right branches) because of the lack of data. The difference in independent estimates of the recurrence curve slope β obtained in three different ways is only around 1.5%.

We see that the model works correctly, but have we learned anything new about the seismic process? We have seen that spatial and energetic scalings of seismic processes are interrelated. The energetic scaling here implies the slope of the recurrence graph. It may seem surprising for seismologists that the slope of the recurrence plot can be found without plotting it, and yet the parameter β can indeed be computed on the basis of the analysis of only the spatial distribution of epicenters and seismic energy (41). The scale invariance turned out to be not an external attribute of seismicity but the structural core of the whole process.

In Ref. [90], the idea of scaling correspondence was extended to include three multifractal fields: fault, seismic, and seismoenergetic (the model of a self-similar self-organized structure of Earth's crust). We note that the question of the connection between seismic activity in the crust with morphologic structures has been discussed for a long time in the seismotectonic literature [94–96]. Traditionally, to find links between disjoint and seismic structures, Euclidian geometry is used: in Earth's crust, some bounded volumes are selected that contain hypocenters of earthquakes related in one way or another to rupture trajectories. No universal description of the relation between seismicity and fault formation was found this way. And yet a solution can be found with the help of fractal geometry. The true relation between multifractal fields is revealed in the correspondence between their scalings.

The relation between the multipliers of multiplicative cascades in the model of scaling correspondence is not limited to a power-law dependence like (35). More general cases are considered in Ref. [93].

4. Microlevel of fracture

4.1 Kinetics of microfractures

Any failure of polycrystalline rock (including earthquakes) begins with the breakup of molecular bonds. Two models were proposed to describe this process, based on completely different premises. The kinetic concept of strength assumes that the breakup occurs when the energy of thermodynamic fluctuations exceeds the bond energy (the activation energy), which leads to a kinetic equation of the form [4, 97]

$$\frac{\mathrm{d}Q}{\mathrm{d}t} \propto \exp\left(-\frac{E-\gamma\sigma}{k_{\mathrm{B}}T}\right), \qquad (42)$$

where Q has the meaning of the number of broken bonds per time t, E is the activation energy, σ is the mechanical stress, T is the absolute temperature, k_{B} is Boltzmann's constant, and γ is a material parameter.

The quantum model, an alternative to the kinetic concept, explains the disappearance of the interaction potential between atoms of a crystal solid body by the tunnel transition of valence electrons from the valence band to the conductivity band or the continuous spectrum [5]. This model leads to the kinetic equation

$$\frac{\mathrm{d}Q}{\mathrm{d}t} \propto \exp\left(-\frac{C}{\sigma}\right), \qquad (43)$$

where C is a material parameter.

Which of these models corresponds to the real fracture process in rock? There is no unique answer yet. However, in their physical essence, Eqns (42) and (43) model the kinetics of the breakup of *different* crystals: Eqn (42) corresponds to the breakup of crystals with ion bonds, whereas Eqn (43) corresponds to the breakup of crystals with covalence bonds.

Most minerals forming the erupted rock are dielectric and are characterized, like most dielectrics, by ion interatomic bonds. Ion bonds require much lower energy to be broken than covalence bonds do. It is therefore reasonable to guess that the mechanism implied by Eqn (42) should be realized in Earth's crust with a higher probability than the mechanism implied by Eqn (43).

Equation (42) is the classical equation of the Arrhenius chemical kinetics [98], adapted to chemical reactions that depend on the presence of mechanical stresses. In other words, the kinetic concept of strength governs the breakup of ion crystals (and hence earthquakes) as a solid-body chemical reaction of dissociation. The mechanical stresses in this case are not the cause but a catalyst of the breakup process (according to Eqn (42), for $\sigma = 0$ but $T \neq 0$, the rate of crack appearance is $\mathrm{d}Q/\mathrm{d}t > 0$). In fact, in agreement with the kinetic concept of strength, earthquakes as an instantaneous release of energy of intermolecular bonds should be considered a chemical ('molecular') explosion. An even more radical conclusion was proposed in [6], associating earthquakes with critical phenomena such as 'a chain chemical explosion' occurring in a 'lithospheric macroreactor'. Taking the goals of this review into account, we note that there are indeed some analogies between chain reactions and the process whereby microcracks coalesce into a macrorupture.

However, both models agree in that the cause of the breakup lies in the nonequilibrium state of the crystal lattice. Just the fluctuations — thermodynamic or quantum — lead to the breakup of molecular bonds. Accordingly, rupture on larger scales inherits the fluctuating character of the source of the fracture.

4.2 Scale invariance at the stage of crack coalescence

The concept of an empirical criterion of crack coalescence was introduced nearly 30 years ago [99]. For cracks of the same length, the coalescence criterion is written as

$$K = \frac{L}{l} = \frac{1}{l\sqrt[3]{X}} \approx \mathrm{e}\,, \qquad (44)$$

where L is the distance between the tips of the cracks, i.e., the size of the barrier that must be overcome when the cracks coalesce, l are the lengths of coalescing cracks, X is the concentration of cracks of the same length in the material, and e is the base of the natural logarithm. According to the definition of the coalescence criterion (called the 'concentration criterion'), cracks coalesce at the same thermodynamic parameters of the medium as those at which cracks form, if the distances between them become approximately equal to e crack lengths. In practice, the coalescence criterion is frequently taken to be three, $K \approx 3$. As follows from definition (44), the spatial distribution of cracks in this case is assumed to be homogeneous. This is explained by the fact that up to the time the coalescence criterion was experimentally discovered, there had been no information in fracture physics about the presence of an internal structure of any kind in ensembles of cracks. Because it was later shown that real spatial distributions of cracks in rock are always fractal, the numerical value of the coalescence criterion must be recalculated in general with this fact taken into account. For example, in experimental work exploring the coalescence process for cracks artificially introduced in rock samples, it has been shown that cracks coalesce under load if the distance between them is equal to their length [100, 101].

However, it is much more important that on a purely experimental level it was found (even before the birth of fractal geometry!) that the criterion of crack coalescence in Eqn (44) has a scale-invariant nature. It is easy to see what the result of the action of the scale-invariant coalescence criterion on a scale-invariant ensemble of cracks is. In Fig. 4, arrow *1* shows a well-known procedure, the first five iterations leading to the Cantor set (a unit interval is split into three equal parts and the middle one is removed; each of the remaining parts is also split into three, with the middle one-thirds removed, and so on). For an infinite number of iterations, this procedure generates a set of the Lebesgue measure 0, 'Cantor dust', or the simplest fractal. We interpret the intervals on the lowest scale level as microcracks, assuming that the scale-invariant coalescence criterion is observed for the nearest microcracks (whatever its numerical value). As soon as the closest cracks of the lowest level coalesce, they become cracks of the coarser scale, but on this new scale level (as well as on all subsequent ones), the coalescence criterion is also satisfied. Hence, the coalescence proceeds as an avalanche ending in a macrorupture.

Arrow *2* in Fig. 4 shows this inverse crack coalescence process. In the framework of a scale-invariant crack distribution and under the action of the scale-invariant coalescence criterion, nothing can stop the fracture avalanche. The process of the avalanche coalescence of microcracks from the microlevel to the macrorupture can be referred to as a 'geometric phase transition', a term borrowed from the percolation theory [102]. The use of such a terminology is fully relevant because the result of a geometric phase transition is an objectively significant change in the material structure: an initially small-scale structure acquires a large-scale order. The procedure of inverse cascade was repeatedly used to model earthquake preparation processes [102–105]. A crack elongation cascade is also observed in laboratory experiments [106].

We return to the schematic in Fig. 4. Let $\aleph$ denote the number of remaining parts of the interval at the second stage of the cascade procedure just described. In general, $\aleph$ can be any natural number: it characterizes the structure of the set, which can have an infinite number of variants. We assume that the distance between the remaining parts is expressed as an integer number of lengths of the remaining parts (interpreted, as previously, as 'cracks'). Then the number of elements in the set of 'cracks' at the kth iteration is expressed as

$$\aleph(k) = \aleph^{k-1}\,, \tag{45}$$

and the length of the elements in our set (the length of 'cracks') can be found from the equation

$$l(k) = \left[\aleph + K(\aleph - 1)\right]^{-(k-1)}\,. \tag{46}$$

We take l as the scale unit $l = 1/\lambda$. Then the fractal dimension of our set can be found as

$$\aleph \propto l^{-d_{\mathrm{f}}}\,. \tag{47}$$

Inserting (45) and (46) into Eqn (47), we find

$$d_{\mathrm{f}} = -\lim_{l\to 0} \frac{\ln \aleph^{k-1}}{\ln\left[\aleph + K(\aleph-1)\right]^{-(k-1)}} = -\frac{\ln \aleph}{\ln\left[\aleph + K(\aleph-1)\right]^{-1}}\,. \tag{48}$$

Hence, for the types of one-dimensional sets considered here (for integer K), if the distance between the remaining parts of the interval corresponds to K, the relation of the coalescence criterion to the fractal dimension of the resulting set becomes

$$K = \frac{\aleph^{1/d_{\mathrm{f}}} - \aleph}{\aleph - 1}\,. \tag{49}$$

Varying the structure number $\aleph$, we can obtain an infinite variety of forms of the 'crack sets' model in the scheme considered. We see that the use of the scale-invariant coalescence criterion in a scale-invariant set of cracks radically changes even the paradigm of fracture (rock fracture is not a stability loss by a single macrocrack but the stability loss in a set of microscopic cracks). This raises a number of unanticipated questions. Even from the rather simple scheme considered here, it becomes clear that cracks can coalesce at many points of the trajectory of future macroruptures. What should then be called the earthquake 'epicenter'? For the fractal spatial distribution of microcracks, their net length Nl, as follows from Eqns (45) and (46), tends to zero,

$$\lim_{\substack{k\to\infty\\ l\to 0}} \frac{\aleph^{k-1}}{\left[\aleph + K(\aleph-1)\right]^{k-1}} = 0\,, \tag{50}$$

i.e., is theoretically an infinitesimal quantity. In other words, do earthquakes evolve from 'nothing'? In a finite scale range, the crack lengths are of course always finite, but expression (50), albeit with some reservations, invites such a hyperbolized metaphor.

Computer simulations show that for sufficiently large $\aleph$ (for example, $\aleph > 10^2$) the number of crack coalescence stages, covering the entire range from microcracks to seismic faults, is very moderate, being less than 10. If the microcracks whose number is sufficient for them to coalesce and form a macrorupture (once again, in a finite scale range) were redistributed uniformly in space, they would be separated by absolutely nonpenetrable barriers of undamaged material.

Figure 4. Arrow *1* shows the first five iterations of the uniform Cantor set construction. For an infinite number of iterations, this procedure generates a simple fractal — a set of the Lebesgue measure 0 with $d_{\mathrm{f}} \approx 0.63$. Arrow *2* shows an inverse cascade procedure — subsequent coalescence of microcracks if the nearest of them satisfy the coalescence criterion K (the intervals are interpreted as microcracks). Thus, via subsequent coalescence events in the scale-invariant set of microcracks, a macrorupture can form.

Microcracks whose number is so small can coalesce into a macrorupture just because they are distributed extremely irregularly in space, i.e., in a scale-invariant manner. We again face scale invariance as an indicator of a critical state in a nonequilibrium system. Related experimental research shows that the ensembles of cracks in rock almost always have a self-similar spatial structure, and hence the accumulation of microcracks in rock is a process of gradual increase in the fractal dimension of microcrack sets continuing to the critical transition — the avalanche coalescence.

The scheme of a geometric phase transition considered above is transparent even on an intuitive level; however, the path from it to quantitative estimates of failure parameters proved to be extremely difficult. Real sets of microcracks exist in rock and are always three-dimensional. We have not yet succeeded in exploring the structure and fractal dimensions of one-dimensional subsets of such three-dimensional sets. Today, we still do not know the critical values of the fractal dimensions of one-dimensional crack ensembles, i.e., the values of fractal dimensions at which cracks coalesce in an avalanche manner into a major rupture, causing a geometric phase transition in rock. And yet, the scheme considered above does not contain ungrounded assumptions and represents generalizations of empirically collected facts; we can therefore hope that it will be elaborated further as new information becomes available.

5. Prognostic criteria of earthquakes

5.1 Spatial distribution of epicenters

So what is the crust earthquake preparation process? We collect the known results of observational, model, and theoretical studies and formulate a cautious phenomenological hypothesis. In the process of tectonic deformation of Earth's crust, because of geometric, structural, or any other inhomogeneity, a concentration of stresses can appear in the crust interior. In the region of stress concentration (having a macroscopic size), the accumulation rate of individual microcracks substantially increases. In the process of further deformation and microcrack accumulation, the region of stress concentration gradually evolves into a strongly nonequilibrium state and approaches an instant when stability is lost. In the region of stress concentration, microcracks form fractal clusters (sets of microcracks with self-similarity of a general form, multifractality). As the cluster monofractal dimension reaches a critical value, an avalanche coalescence of cracks into a macrorupture is initiated (a geometric phase transition), which is what is regarded as an earthquake on Earth's surface.

We stress that it is only a hypothesis, which is intentionally formulated in a purely schematic way. But it does not contradict any known facts, and therefore invites some general conclusions.

First, the 'source' of a forming earthquake is a fractal cluster of microcracks, having no characteristic size, shape, envelope surface, or characteristic scale. Second, as an earthquake forms, no intermediate physical mechanisms are required on mesoscales between the microscopic cracks caused by thermodynamic fluctuations and the macrorupture (for example, 'trigger' actions like fluid diffusion). Owing to the scale invariance of a microcrack cluster, the cascade of fracturing overcomes any scale range. And third, processes leading to earthquakes occur in any crystalline rock fragment, irrespective of its size. The cause of failure is the nonequilibrium state of the crystal lattice in and of itself. A natural failure is perceived as seismicity if the 'rock fragment' becomes very large, for example, reaches the size of a lithospheric plate, and the rupture reaches 'seismic' scales because of its scale invariance.

The analysis could be continued, and each of the questions touched on here discussed, but our intention is now to find which processes preceding an earthquake can be diagnosed from the surface of Earth and used as prognostic indicators of an earthquake that is about to occur. We cannot measure stresses at the 'source', we cannot see the appearance of microcracks there, and we cannot measure the fractal dimensions of microcrack clusters. But we can assume that given a highly inhomogeneous distribution of microcracks in a three-dimensional rock, the fractal dimension of a microcrack set do not reach critical values at different points in the region of stress concentration simultaneously. The formation of a major rupture (global loss of stability) must be preceded by a smaller-scale seismicity.

If, using the terminology of the theory of dissipative structures, we consider an earthquake as a global 'bifurcation' in the process of seismogenic system evolution, then, based on very general arguments, we can expect that 'bifurcations' in a strongly nonequilibrium state are preceded by growing 'fluctuations' in system parameters. In our case, this implies fluctuations in seismic activity. That said, detecting and distinguishing them against the extremely irregular the background seismic activity is a problem far from trivial.

We can try to solve this problem by methods of the multifractal theory. An additional difficulty is brought about by low representability of the existing seismic data. The threshold of representability of seismic data is rather high today, commonly up to two magnitude units. The amount of data is simply insufficient to be used for constructing multifractal measures (seismic fields), for example, monthly. If they are constructed based on data for several years, the result are cumulative fields that lack information on the time of particular fluctuations of seismic activity. However, we can at least try to detect their presence.

To test these assumptions (in hindsight) we apply the following computational procedure. We take the data of a seismic catalog preceding strong earthquakes in the vicinities of their epicenters for 4–5 year, split these data into two samples over time intervals of 2–2.5 years, and construct two multifractal fields based on these samples. One then characterizes the seismic activity of the vicinity of the future epicenter long before the strong earthquake, while the other does it directly before. In this manner, we model seismic fields of the steady state and the transient process before a strong earthquake. If the methods of multifractal analysis are sensitive to the fluctuations of seismic activity, the parameters of model fields should differ.

The results of such a comparison are presented in Fig. 5 [107, 108]. The singularity spectra of seismic fields constructed from the data on seismicity in an 80×80 km^2 region before the Joshua Tree earthquake in southern California (23.04.1992, magnitude $M = 6.1$, depth of hypocenter 12 km) are shown in Fig. 5a. The epicenter of this earthquake was at the center of the region. The first spectrum (solid curve) is based on the data for the period 01.04.1988–01.04.1990 (1713 events) and the second one (dashed curve) used data from 01.04.1990–23.04.1992 (1713 events).

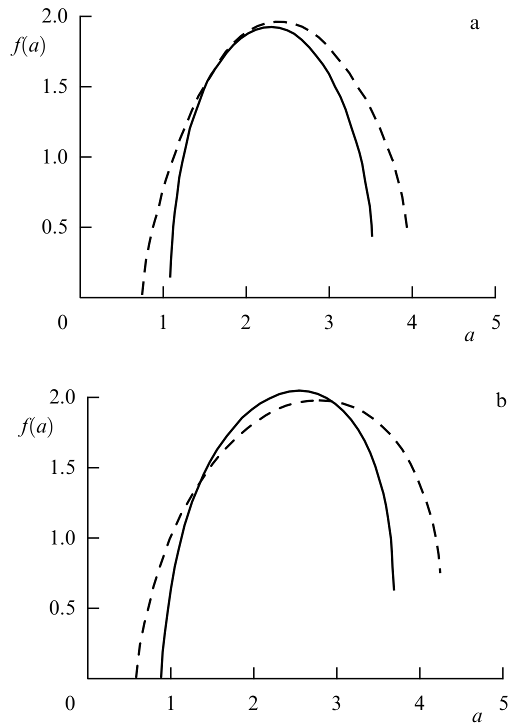

Figure 5. Effect of widening of the $f(a)$ spectra of seismic fields prior to (a) the Joshua Tree earthquake (1992, $M = 6.1$) in southern California, (b) an earthquake in Iceland (2000, $M = 6.6$). The wider spectra (dashed curves) are based on the data from two years before these earthquakes, while the narrower spectra (solid curves) rely on earlier data.

Figure 5b shows spectra of seismic field singularities based on seismicity data in a 60×60 km^2 area before an earthquake in Iceland (17.06.2000, $M = 6.6$, depth of hypocenter 6.3 km). The first spectrum (solid curve) is based on data from 28.05.1995–17.06.1998 (2230 events), and the second one (dashed curve) is based on data for the period 17.06.1998–17.06.2000 (2230 events).

Figure 5 shows that in both cases the $f(a)$ spectra of seismic fields based on the seismicity data preceding strong earthquakes turn out to be substantially broader than those characterizing earlier seismic activity. Seismic fields that directly precede strong earthquakes contain wider ranges of singularity indices, which quantitatively (statistically) reflects the presence of fluctuations in seismic activity before strong earthquakes (short-term but substantial bursts in seismic activity at some points and reduction in activity at others). It can be assumed that broadening in the $f(a)$ spectra of seismic fields is caused by the transition of seismogenic systems into a strongly nonequilibrium state before they lose their stability (before the main shocks of earthquakes or system breakup).

We note that the process conductive to strong earthquakes is revealed through the analysis of higher moments of multifractal measures constructed from seismic data, whereas the monofractal dimensions of these measures (the values of spectral extrema) are only weakly sensitive to rearrangements in the field structure. The reason is that a large number of earthquakes occur at the same field points (at focal centers), which induce the earthquakes many times. Precisely the distribution of focal centers determines the monofractal field dimensions, and these distributions are stationary (because they are tightly connected to the fault fields). The variable quantity is the seismic activity of focal centers, which is reflected in the behavior of the higher moments of measures. Taking the already mentioned thermodynamic analogs in the theory of multifractal measures into account, seismic scaling can be called the macroparameter of the seismogenic medium, which, like temperature in a thermodynamic system, allows diagnosing the state of a seismogenic system and the degree of its closeness to the moment it loses global stability.

5.2 Temporal course of seismicity

The effect of widening of the $f(a)$ spectra of seismic fields before strong earthquakes points explicitly to changes in a seismic process with time and to the presence in this process of steady-state and transient regimes, which ends with a strong earthquake (we refer to a 'strong' earthquake only because the sensitivity of present-day seismic networks does not allow this effect to be seen prior to the 'weak' events). We have already mentioned that the evolution of seismicity with time can be self-similar. We now explore this question in more detail.

The behavior of any dynamic system in a steady state can be studied by constructing its attractor (phase portrait), i.e., the limit subset in phase space that determines the sequence of system states (phase trajectory). The construction of an attractor does not cause any problems if the system evolution equations are known. However, for seismicity we know neither the evolution equations nor their number. In such situations, the topological invariants of the attractor of a dynamical system can be computed with the help of an attractor reconstruction procedure based on the temporal behavior of an experimentally observed system parameter. This procedure relies on the proof of a theorem by Tackens [109].

The procedure of attractor reconstruction by a seismic time series is carried out in Ref. [110]. As this series, a series is taken whose elements are the numbers of events per unit of astronomic time. The data of the South Californian catalogue were used for the region to the south of the Salton Sea in southern California, bounded by a circle 25 km in radius. Strong earthquakes are not known for this region, for both instrumental and historical periods, which allows us to refer to the seismic regime that is studied as a steady-state one. The sample consisted of data on 3398 events in the magnitude range $1.7 \leqslant M \leqslant 5.1$ for the period from 01.01.2000 to 01.11.2014.

The reconstruction has shown that the seismic attractor was a strange chaotic attractor in a three-dimensional phase space. An estimate for the largest Lyapunov exponent gave a positive value for it, which is a criterion of chaos. Thus, it was shown that the temporal course of seismic kinetics in the steady state is chaotic and unpredictable. The time series in this case does not contain information on the concrete state of the system in the future; it only contains statistical information on the topological structure of the attractor. The seismic time series in a steady state does not have scale invariance either.

To be fair, we must mention that proposals for the Poisson character of seismic time series were formulated long ago [111]. Our task, however, is to find prognostic indicators of strong earthquakes in the time series of seismicity, and once again a 'signal' has to be singled out from the 'background' characterized by extremely high intermittency.

But we first reflect on whether a seismic time series, each element of which represents the number of seismic events per unit of astronomical time, is the best characteristic of the time evolution of the process of seismic kinetics. When constructing a traditional seismic time series, one is forced to select a sufficiently large time unit (of the order of a month) in order to avoid the appearance of null (no-content) elements. In this case, information on the time of particular events is lost, while the total number of elements in the series in many cases proves to be insufficient for statistical analysis. Thus, we are prompted to seek a method of handling the temporal seismic data that would preserve all the information on times of seismic events contained in catalogs.

The analysis of a series whose elements are the intervals between subsequent seismic events in the region where the earthquake is about to occur (the focal area) [112] can be proposed as such a method. The size of the focal area is routinely computed using the Sadovskii formula [113], which can be written as

$$\mathfrak{J} \approx \sqrt[3]{\frac{E}{10^3}}\,, \tag{51}$$

where E is the earthquake energy [erg] and $\mathfrak{J}$ is the linear size of the focal area [cm]. In particular, for an earthquake with $M = 7$, formula (51) gives $\mathfrak{J} \approx 3 \times 10^6$ cm = 30 km.

In the original study by Sadovskii [113], the quantity $\mathfrak{J}^3$ is treated as the 'source' volume. However, according to the phenomenological scheme in Section 5.1, the 'source' is the fractal cluster of microcracks for which the notion of volume is not applicable. In the framework of this scheme, $\mathfrak{J}$ can be interpreted as a size proportional to the gyration radius R_g [114, 115] for a fractal cluster of microcracks,

$$\mathfrak{J} \propto 2R_g\,, \tag{52}$$

where

$$R_g = \left(\frac{1}{N_*}\sum_{i=1}^{N_*}\left|\mathbf{r}_i - \mathbf{r}_{\mathrm{CM}}\right|^2\right)^{1/2}. \tag{53}$$

Here, $\mathbf{r}_{\mathrm{CM}}$ is the radius vector of the barycenter of the cluster, $\mathbf{r}_i$ are the radius vectors of the cluster elements, and N_* is the net number of cluster elements. The gyration radius is 'the root-mean-square cluster radius' and, in all probability, a plausible characteristic of the 'source' that represents a fractal set of microcracks. A circle with the radius equal to the gyration radius embraces the dominant number of cluster elements, which, as applied to seismology, means the dominant number of earthquake aftershocks (if they are observed). The major rupture is approximately located within this circle.

We turn once again to the South California catalog. The last of the strongest earthquakes that took place in southern California (more precisely, on Mexican territory) is the Northern Baja or Sierra Mayor Cucapah earthquake, 04.04.2010, $M = 7.2$, with the depth of hypocenter 10 km. For the focal area of this earthquake with a radius of 15 km ($\mathfrak{J}/2$) for the period 01.01.1990–04.04.2010, the catalog reports data on 2991 events with a magnitude exceeding the threshold one, $M \geqslant 1.7$ ($M = 1.7$ is the representativeness threshold for the catalog). We enumerate the events in the sampling explored by the index i in the direction of increasing time. Then the time interval between events with indices i and $i + 1$ is

$$\Delta t_i = t_{i+1} - t_i\,, \tag{54}$$

where t_i is the time of the ith event.

Figure 6a shows a series of time intervals Δt_i constructed for the sampling considered after cleaning the data from aftershocks. The figure shows that the series Δt_i is a numerical series that can be formally treated as a geometrical object, i.e., as a distribution of time intervals over the uniform axis of their listing indices or as the distribution of the measured physical parameter over a uniform scale grid. Such a representation of the catalog data has characteristic features that make it distinct from traditional seismic time series (whose elements are the numbers of events per unit time). As mentioned above, in traditional time series, information on the time of particular events is lost, whereas it is preserved in the series of time intervals Δt_i and can be directly used in computations. The number of elements of the time interval series is sufficiently large for statistical analysis. The values of Δt_i can be determined with high accuracy because the astronomical time of seismic events is recorded up to

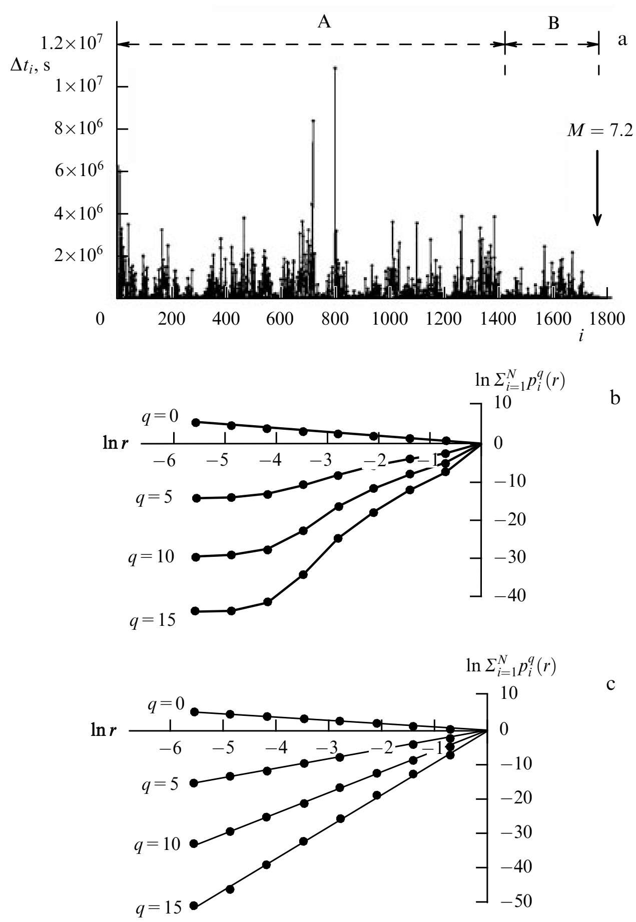

Figure 6. Emergence of self-similarity in the temporal behavior of microseismicity in the focal region of the Northern Baja earthquake (2010, $M = 7.2$). (a) A series of time intervals between subsequent microearthquakes that took place in the focal area. The abscissa plots the ordering number of events, the ordinate plots the duration of the time interval in seconds. The arrow points to the moment of the Northern Baja earthquake. The values of series elements are shown by dots, which are connected by lines to guide the eye. (b) The dependence of the sum of measure moments on the scale for the main part of the series (A). (c) The dependence of the sum of measure moments on the scale for the final part of the series (B).

seconds. As we can see, the series of intervals Δt_i preserves practically all temporal information about the process of seismic kinetics present in the catalog.

The analysis of time interval series amounted to a numerical data filtration in a running window, with the use of scaling analysis methods. The running window (of the size of n elements of the series) was moved along the axis of natural indices for the elements of the series Δt_i being explored. The elements of the series that fit inside the running window were transformed to the measure P, whose fractions p_j related to a single element of the series were approximated with the help of normalization. In this way, the measure P was distributed over a uniform grid of n boxes. Further, the validity of a power-law relation between the distribution function and the scale (or a linear relation between their logarithms, which is the same) Eqn (6), was tested. The values of q and r were discretized. The scale variations r $(r = r_1, r_2, \ldots, r_{\min})$ were set by the grid renormalization, and the values of q were stepped through the intervals $\Delta q = 0.1$ in a finite range of values. For a fixed value of q, the matrices

$$Y_q = \left(\mathbf{X}_{r1}\ \ \mathbf{X}_{r2}\ \ \ldots\ \mathbf{X}_{r_{\min}}\right)^{\mathrm{T}} \tag{55}$$

were constructed, with their rows being the vectors

$$\mathbf{X}_r = \left[\ln\left(\sum_{j=1}^{N} p_j^q(r)\right), \ln r\right]. \tag{56}$$

Resorting to the components of matrices (55), the dependences of $\ln\left(\sum_{j=1}^{N} p_j^q(r)\right)$ on $\ln r$ were constructed, which could be linear [with valid relation (6)] or nonlinear [with relation (6) violated]. The computations were then repeated for the next value of q.

For the convenience of the scaling analysis, the size of the running window was chosen equal to $n = 2^8 = 256$ series elements, i.e., the renormalization of the measure P was carried out with the use of a binomial cascade scheme. On finishing particular computations, the window was shifted along the series by one element and the full cycle of computations was repeated. In this way, the variability in the series was explored along its entire length.

Figure 6a shows that the series of time intervals can be split into two parts: the main one (A) and the final one (B). Over the entire length of the main part, the dependences of the sum of measure moments on the scale had a shape resembling that in Fig. 6b. As we can see, the dependences of $\ln\left(\sum_{j=1}^{N} p_j^q(r)\right)$ on $\ln r$ for part (A) of the series are nonlinear — relation (6) is not satisfied for them. Thus, no structure is observed in part (A) of the series. It is noteworthy that the nonlinearity of the dependences of $\ln\left(\sum_{j=1}^{N} p_j^q(r)\right)$ on $\ln r$ increases with the moment order q: the analysis of higher moments allows identifying the main part of the series as a chaotic one (the sensitivity of lower moments to chaos is substantially lower). We thus reproduced the result obtained in reconstructing the seismic attractor: the temporal course of the seismic kinetics is chaotic in a steady state.

However, in the final (B) part of the series, the dependences of $\ln\left(\sum_{j=1}^{N} p_j^q(r)\right)$ on $\ln r$ become linear, i.e., the series acquires a statistically self-similar structure (Fig. 6c). As can be seen, prior to the Northern Baja earthquake, scale invariance emerged in the structure of the series studied.

Thus, the process of seismic kinetics in the focal region of the Northern Baja earthquake was characterized by chaotic features over a long time period, but approximately 21 months prior to the main shock a global scale-invariant structure began to form in the temporal course of microseismicity (within the focal region). It is natural to assume that the cause of this was the global (on the scale of the focal region) transition of the material in Earth's crust into a strongly nonequilibrium state, which then culminated in the main shock of the Northern Baja earthquake. The transition was accompanied by the appearance of statistical self-similarity in the temporal course of microseismisity, which could be detected and revealed by multifractal analysis methods, when the scale-invariant series structure was formed over a scale interval sufficiently wide for numerical analysis. Therefore, the appearance of self-similarity in the series of time intervals between sequential events can be considered a physically grounded prognostic indicator of strong earthquakes.

As an additional result, we note that in the main part of the series (A), the sample mean for the duration of the time interval was 406529.01... s, whereas in the final series, part (B), the sample mean of the interval length turned out to be equal to 181308.29... s, i.e., smaller by more than two times. Part (B) of the series directly preceding the main shock of the Northern Baja earthquake is the one with shorter ('on average') time intervals Δt_i relative to the main-series part (but strong intermittency, which is characteristic of the whole series, is preserved).

In accordance with the SOC concept and the dissipative structure theory, the temporal scale invariance of the seismic kinetic process reveals a strongly nonequilibrium medium state. Therefore, we can note certain analogies between the structural organization of the series of time intervals Δt_i and properties of the internal time in nonequilibrium systems introduced by Prigogine [12] in the theory of dissipative structures. As mentioned, the internal time coincides with the astronomical time on average, but can deviate from it in periods of instability. As indicated by the study carried out, systematic deviations of the durations of time intervals Δt_i from the sample-mean value $\langle \Delta t \rangle$ over the main part of the series were indeed observed shortly before a strong earthquake, when the seismogenic system was in a critical state. It can be speculated that the length of time intervals Δt_i is sensitive to the same physical factors as is the internal time of a nonequilibrium system according to Prigogine. The main factors are the change in the thermodynamic entropy of the system and the degree of system closeness to the instant of stability loss. As a result of the action of these factors, microearthquakes start to occur 'more frequently', forming a scale-invariant structure in time.

6. Conclusions

Seismicity is one of the most apparent examples of self-organization in complex nonequilibrium systems through a sequence of bifurcations, which leads to a scale-invariant organization of dissipative structures. Numerous mechanical manifestations of seismicity, such as the motion of the sides of a seismic fault and generation of seismic waves, are the macroscopic consequences of thermodynamic processes unfolding at the level of a crystal lattice: the change in system entropy, thermodynamic fluctuations, breakup of molecular bonds, accumulation of microcracks, spatial organization of microcracks in the form of self-similar sets, critical transitions in their structure, and so on. With such a highly extended range between scales of the observed processes and scales of their underlying causes, Nature nevertheless left seismologists a way to obtain direct information on the processes giving rise to earthquakes in real time, and this way is the scale-invariance of seismic processes. Owing to the scale invariance, we understand (at least qualitatively) what happens in Earth's crust on the macro- and microlevels and can detect the period of the unstable, strongly nonequilibrium state in the crustal material that ends with an earthquake.

This review gives examples of how the scale invariance of rock failure occurs, where and how it is observed, which forms it takes, and how it can be used in seismic prognosis. The results of theoretical, experimental, and model studies exploring the scale invariance of seismicity mutually augment each other and allow us to draw a self-consistent picture of earthquake preparation, even if this picture is unconventional from the classical physics standpoint. The scale invariance can be termed the structural bone of seismicity, tightly connected with its physical basis. Seismic scaling is simultaneously a form of nontrivial description of seismic process, the medium macroparameter, and an indicator of its critical state.

The reality of scale invariance of seismic structures in all probability implies that the seismogenic system should be conceived of as a principally nonintegrable one. The main physicochemical phenomenon intrinsic in the process of any crust earthquake evolution is the system self-organization caused by its nonequilibrium state. Self-organization determines the properties of the system as it evolves to the instant of stability loss. In this framework, the earthquake source turns out to be the fractal cluster of microcracks caused by thermodynamic fluctuations, i.e., an object that cannot be explored with the methods of Euclidean geometry. However, such a source model (thus far a hypothetical one) allows explaining a number of specific features built in seismic process , such as the known uncertainties in determining the coordinates of earthquake sources, the impossibility of detecting an earthquake source with seismic sounding methods, and so on. The idea of critical transition (geometric phase transition) in a fractal cluster of microcracks eliminates the question of 'trigger action' at the source, which is frequently proposed to be water diffusion, and therefore the model in the form of a microcrack cluster is applicable to studying not only terrestrial but also lunar seismicity.

Spatial self-similarity of seismic structure is tightly connected with the spatial self-similarity of fault systems in Earth's crust, evolving on geological, not seismic, time scales. This is why the monofractal dimensions of seismic fields are only weakly sensitive to the processes of preparation of separate earthquakes. However, the increase in seismic activity fluctuations prior to 'global bifurcation', predicted by the dissipative system theory, can be detected by the behavior of the higher moments of multifractal measures induced by the sets of epicenters.

Scale invariance is also discovered in the temporal course of the seismic kinetic process in focal areas of future earthquakes. The emergence of scale invariance in the temporal course of seismicity can be seen as a result of the transitional process from a steady state (a chaotic one, characterized by a strange chaotic attractor) to the earthquake proper (the loss of global stability by the system). Thus, the detection of scale invariance in temporal structures of seismicity allows identifying the period when the state of a seismogenic system is strongly nonequilibrium.

The present level of structural studies of seismicity is still limited by a critical and frequently catastrophic lack of data. With an increase in the quality of seismic data, we can also hope that studies of fine structures of seismic objects will become possible, which will eventually lead to new prognostic characteristics of earthquakes. Studies of the fractal structure of seismicity have started, in essence, relatively recently, but their results suggest optimism in looking for new discoveries in the nearest future.

References

1. Sobolev G A *Osnovy Prognoza Zemletryasenii* (Basics of Earthquake Prognosis) (Moscow: Nauka, 1993)
2. Sobolev G A *Kontseptsiya Predskazuemosti Zemletryasenii na Osnove Dinamiki Seismichnosti pri Triggernom Vozdeistvii* (The Concept of Earthquake Predictability on the Basis of Seismicity Dynamics under Trigger Action) (Moscow: IFZ RAN, 2011)
3. Kostrov B V *Principles of Earthquake Source Mechanics* (Cambridge: Cambridge Univ. Press, 1988); Translated from Russian: *Mekhanika Ochaga Tektonicheskogo Zemletryaseniya* (Moscow: Nauka, 1975)
4. Zhurkov S N *Vestn. Akad. Nauk SSSR* (3) 46 (1968)
5. Gilman J J, Tong H C *J. Appl. Phys.* **42** 3479 (1971)
6. Buchachenko A L *Phys. Usp.* **57** 92 (2014); *Usp. Fiz. Nauk* **184** 101 (2014)
7. Arnold V I *Catastrophe Theory* (Berlin: Springer-Verlag, 1992); Translated from Russian: *Teoriya Katastrof* (Moscow: Nauka, 1990)
8. Thompson J M T *Instabilities and Catastrophes in Science and Engineering* (Chichester: Wiley, 1982); Translated into Russian: *Neustoichivosti i Katastrofy v Nauke i Tekhnike* (Moscow: Mir, 1985)
9. Mandelbrot B *PAGEOPH* **131** 5 (1989)
10. Schertzer D, Lovejoy S *Physica A* **185** 187 (1992)
11. Prigogine I *The End of Certainty. Time, Chaos, and the New Laws of Nature* (New York: The Free Press, 1997); Translated into Russian: *Konets Opredelennosti. Vremya, Khaos i Novye Zakony Prirody* (Moscow–Izhevsk: RKhD, 1999)
12. Prigogine I *From Being To Becoming. Time and Complexity in The Physical Sciences* (San Francisco: W.H. Freeman and Co., 1980); Translated into Russian: *Ot Sushchestvuyushchego k Voznikayushchemu. Vremya i Slozhnost' v Fizicheskikh Naukakh* (Moscow: Editorial URSS, 2002)
13. Guglielmi A V *Phys. Usp.* **58** 384 (2015); *Usp. Fiz. Nauk* **185** 415 (2015)
14. Bak P, Tang C J *Geophys. Res.* **94** 635 (1989)
15. Grassberger P *Phys. Lett. A* **97** 227 (1983)
16. Meneveau C, Sreenivasan K R *Phys. Rev. Lett.* **59** 1424 (1987)
17. Vicsek T, Family F *Phys. Rev. Lett.* **52** 1669 (1984)
18. Kohomoto M, Technical Report of ISSP. Ser. A No. 2014 (Tokyo: Univ. of Tokyo, 1988)
19. Kagan Y Y *Nonlin. Sci. Today* **2** 8 (1992)
20. Prigogine I *Acad. R. Belg. Bull. Cl. Sci.* **31** 600 (1945)
21. Klimontovich Yu L *Sov. Tech. Phys. Lett.* **9** 606 (1983); *Pis'ma Zh. Tekh. Fiz.* **9** 1412 (1983)
22. Bak P, Tang C, Wiesenfeld K *Phys. Rev. A* **38** 364 (1988)
23. Grinstein G, in *Scale Invariance, Interfaces, and Non-Equilibrium Dynamics* (NATO ASI Series, Ser. B, Vol. 344, Eds A McKane et al.) (New York: Plenum Press, 1995) p. 261
24. Caruso F et al. *Phys. Rev. E* **75** 055101(R) (2007)
25. Zhang Y-C *Phys. Rev. Lett.* **63** 470 (1989)
26. Sornette A, Sornette D *Europhys. Lett.* **9** 197 (1989)
27. Yang X, Du S, Ma J *Phys. Rev. Lett.* **92** 228501 (2004)
28. Steacy S J et al. *Geophys. Res. Lett.* **23** 383 (1996)
29. Pruessner G *Self-Organised Criticality: Theory, Models, and Characterisation* (Cambridge: Cambridge Univ. Press, 2012)
30. Dhar D *Physica A* **369** 29 (2006)
31. Mandelbrot B B *The Fractal Geometry of Nature* (San Francisco, Calif.: W.H. Freeman, 1982)
32. Frisch U, Parisi G, in *Turbulence and Predictability in Geophysical Fluid Dynamics and Climate Dynamics* (Proc. of the Intern. School

of Physics "Enrico Fermi", Course 88, Eds M Ghil, R Benzi, G Parisi) (Amsterdam: North-Holland, 1985) p. 84
33. Halsey T C et al. *Phys. Rev. A* **33** 1141 (1986)
34. Schertzer D, Lovejoy S *J. Geoph. Res. D* **92** 9693 (1987)
35. Lovejoy S, Schertzer D *Water Resour. Res.* **21** 1233 (1985)
36. Wilson K G *Rev. Mod. Phys.* **55** 583 (1983)
37. Chhabra A B et al. *Phys. Rev. A* **40** 5284 (1989)
38. Atmanspacher H, Scheingraber H, Wiedenmann G *Phys. Rev. A* **40** 3954 (1989)
39. Gibbs J W *Trans. Connect. Acad.* (2) 382 (1873); Translated into Russian: *Termodinamika, Statisticheskaya Fizika* (Moscow: Nauka, 1982) p. 40
40. Bale H D, Schmidt P W *Phys. Rev. Lett.* **53** 596 (1984)
41. Jouini M S, Vega S, Mokhtar E A *Nonlin. Process. Geophys.* **18** 941 (2011)
42. Radlinski A P et al. *J. Appl. Crystallogr.* **33** 860 (2000)
43. Sen D, Mazumder S, Tarafdar S *J. Mater. Sci.* **37** 941 (2002)
44. Wong P, Howard J, Lin J-S *Phys. Rev. Lett.* **57** 637 (1986)
45. Hirata T, Satoh T, Ito K *Geophys. J. Int.* **90** 369 (1987)
46. Chelidze T, Gueguen Y *Int. J. Rock Mech. Mining Sci.* **27** 223 (1990)
47. Feng X-T, Seto M *Geophys. J. Int.* **136** 275 (1999)
48. Johansen A, Sornette D *Eur. Phys. J. B* **18** 163 (2000)
49. Turcotte D L, Newman W L, Shcherbakov R *Geophys. J. Int.* **152** 718 (2003)
50. Sammis C G, Biegel R L *PAGEOPH* **131** 255 (1989)
51. Badri A et al. *Acta Stereol.* **13** 183 (1994)
52. Shao S-M, Zou J Ch *Acta Seismol. Sin.* **9** 485 (1996)
53. Krylov S S, Bobrov N Yu *Fraktaly v Geofizike* (Fractals in Geophysics) (St. Petersburg: Izd. St.-Peterburgskogo Univ., 2004)
54. Hirata T *PAGEOPH* **131** 157 (1989)
55. Vignes-Adler M, Le Page A, Adler P M *Tectonophysics* **196** 69 (1991)
56. Stakhovsky I R, Belousov T P *J. Earthquake Prediction Res.* **5** 505 (1996)
57. Stakhovsky I R, in *Basement Tectonics 11. Europe and Other Regions* (Proc. of the Intern. Conf. on Basement Tectonics, Vol. 5, Eds O Oncken, C Janssen) (Dordrecht: Kluwer Acad., 1996) p. 101
58. Ouillon G, Castaing C, Sornette D *J. Geophys. Res.* **101** 5477 (1996)
59. Tessier Y, Lovejoy S, Schertzer D *J. Appl. Meteorol.* **32** 223 (1993)
60. Boufadel M C et al. *Water Resour. Res.* **36** 3211 (2000)
61. Kagan Y Y, Knopoff L *Geophys. J. Int.* **62** 303 (1980)
62. Geilikman M B, Golubeva T V, Pisarenko V F *Dokl. Akad. Nauk SSSR* **310** 1335 (1990)
63. Hirabayashi T, Ito K, Yoshii T *Math. Seismology* **40** 102 (1990)
64. Ito K, Matsuzaki M *J. Geophys. Res.* **95** 6853 (1990)
65. Hooge C et al. *Fractals* **2** 445 (1994)
66. Lei X, Kusunose K *Geophys. J. Int.* **139** 3 754 (1999)
67. Godano C et al. *Geophys. J. Int.* **136** 99 (1999)
68. Carpineri A, Chiaia B, Invernizzi S *Chaos Solitons Fractals* **14** 917 (2002)
69. Zamani, Agh-Atabai M *J. Sci. Technol.* **39** 521 (2011)
70. Pastén D et al. *Phys. Rev. E* **84** 066123 (2011)
71. Telesca L, Lapenna V, Macchiato M *Physica A* **354** 629 (2005)
72. Telesca L, Toth L *Physica A* **448** 21 (2016)
73. Godano C, Caruso V *Geophys. J. Int.* **121** 385 (1995)
74. Godano C, Alonzo M L, Vilardo G *PAGEOPH* **149** 375 (1997)
75. Wang J-H *J. Geol. Soc. China* **39** 117 (1996)
76. Stakhovsky I R *Fiz. Zemli* (4) 41 (2000)
77. Telesca L, Lapenna V *Tectonophysics* **423** (1 – 4) 115 (2006)
78. Wilson K G *Sci. Am.* **241** (2) 158 (1979)
79. Louis E, Guinea F *Europhys. Lett.* **3** 871 (1987)
80. Louis E, Guinea F *Physica D* **38** 235 (1989)
81. Hassold G N, Srolovitz D J *Phys. Rev. B* **39** 9273 (1989)
82. Hinrichsen E L, Hansen A, Roux S *Europhys. Lett.* **8** 1 (1989)
83. Herrmann H J *Physica A* **163** 359 (1990)
84. Stakhovsky I R *Fiz. Zemli* (11) 11 (1998)
85. Scheidegger A E *Can. J. Phys.* **35** 4 (1957)
86. Turcotte D L, in *Fractals and Dynamic Systems in Geoscience* (Ed. J H Kruhl) (Berlin: Springer-Verlag, 1994) p. 7
87. Turcotte D L *Rep. Prog. Phys.* **62** 1377 (1999)
88. Obukhov A *J. Geophys. Res.* **67** 3011 (1962)
89. Kolmogorov A N *J. Fluid Mech.* **13** 82 (1962)
90. Stakhovsky I R *Izv. Phys. Solid Earth* **43** 1012 (2007); *Fiz. Zemli* (12) 35 (2007)
91. Kulabukhov S Yu *Diskretnaya Matematika* (Discrete Mathematics) (Taganrog: Min. Obshch. Prof. Obr. RF, 2001)
92. Stakhovsky I R *Izv. Phys. Solid Earth* **40** 927 (2004); *Fiz. Zemli* (11) 38 (2004)
93. Stakhovsky I R *Izv. Phys. Solid Earth* **37** 547 (2001); *Fiz. Zemli* (7) 21 (2001)
94. San'kov V A et al. *Razlomy i Seismichnost' Severo-Muiskogo Geodinamicheskogo Poligona* (Faults and Seismicity of the North-Muysk Geodynamic Polygon) (Exec. Ed. S I Sherman) (Novosibirsk: Nauka, 1991)
95. Scholz C H, in *Spontaneous Formation of Space-Time Structures and Criticality* (NATO ASI Series C, Vol. 349, Eds T Riste, D Sherrington) (Dordrecht: Kluwer Acad., 1991) p. 41
96. Reisner G I et al. "Tipizatsiya zemnoi kory i sovremennye geologicheskie protsessy" ("Earth crust types and geological processes at present"), in *Rezul'taty Kompleksnogo Izucheniya Tektonosfery* (Results of Comprehensive Reseach of Earth Techtonics) (Moscow: IFZ RAN, 1993) p. 1
97. Zhurkov S N *Int. J. Fracture Mech.* **1** 311 (1965)
98. Stiller W *Arrhenius Equation and Non-Equilibrium Kinetics*: *100 Years Arrhenius Equation* (Leipzig: BSB B.G. Teubner, 1989); Translated into Russian: *Uravnenie Arreniusa i Neravnovesnaya Kinetika* (Moscow: Mir, 2000)
99. Zhurkov S N et al., in *Fizicheskie Protsessy v Ochagakh Zemletryasenii* (Physical Processes in Earthquake Sources) (Exec. Ed. M A Sadovskii, V I Myachkin) (Moscow: Nauka, 1980) p. 78
100. Shamina O G *Model'nye Issledovaniya Fiziki Ochaga Zemletryasenii* (Model Studies of Physics of Earhquake Sources) (Moscow: Nauka, 1981)
101. Sobolev G A, Kol'tsov A V *Krupnomasshtabnoe Modelirovanie Podgotovki i Predvestnikov Zemletryasenii* (Large-scale Modeling of Preparation of Forerunners of Earthquakes) (Moscow: Nauka, 1988)
102. Stakhovsky I R *Izv. Phys. Solid Earth* **44** 570 (2008); *Fiz. Zemli* (7) 58 (2008)
103. Gabrielov A et al. *Geophys. J. Int.* **143** 427 (2000)
104. Zaliapin I, Keilis-Borok V, Ghil M *J. Stat. Phys.* **111** 815 (2003)
105. Zaliapin I, Keilis-Borok V, Ghil M *J. Stat. Phys.* **111** 839 (2003)
106. Tomilin N G, Kuksenko V S *Fiz. Zemli* (10) 16 (2004)
107. Stakhovsky I R *Izv. Phys. Solid Earth* **38** 156 (2002); *Fiz. Zemli* (2) 74 (2002)
108. Stakhovsky I R *Izv. Phys. Solid Earth* **48** 829 (2012); *Fiz. Zemli* (11 – 12) 47 (2012)
109. Takens F *Lecture Notes Math.* **898** 366 (1981)
110. Stakhovsky I R *Izv. Phys. Solid Earth* **52** 740 (2016); *Fiz. Zemli* (5) 120 (2016)
111. Gardner J K, Knopoff L *Bull. Seismol. Soc. Am.* **64** 1363 (1974)
112. Stakhovsky I R *Put' Nauki* (2) 134 (2016)
113. Sadovskii M A *Dokl. Akad. Nauk SSSR* **275** 1087 (1984)
114. Kolesnichenko A V, Marov M Ya, Preprint No. 75 (Moscow: M.V. Keldysh IPM, 2014)
115. Mikhailov E F, Vlasenko S S *Phys. Usp.* **38** 253 (1995); *Usp. Fiz. Nauk* **165** 263 (1995)